SYNTHESIS AND SINTERING OF TRANSLUCENT YTTRIUM ALUMINIUM GARNET

A THESIS SUBMITTED IN PARTIAL FULFILLMENT

OF THE REQUIREMENT FOR THE DEGREE OF

Master of Technology

in

Ceramic Engineering

Submitted by

Georgekutty Ulahannan

(Roll no: 212CR2498)

Department of Ceramic Engineering

National Institute of Technology

Rourkela

MAY-2014

SYNTHESIS AND SINTERING OF TRANSLUCENT YTTRIUM ALUMINIUM GARNET

A THESIS SUBMITTED IN PARTIAL FULFILLMENT

OF THE REQUIREMENT FOR THE DEGREE OF

Master of Technology

in

Ceramic Engineering

Submitted by

Georgekutty Ulahannan

(Roll no: 212CR2498)

Under the supervision of

Dr. Debasish Sarkar

Department of Ceramic Engineering

National Institute of Technology

Rourkela

MAY-2014

National Institute Of Technology

Rourkela

CERTIFICATE

This is to certify that the thesis entitled "**Synthesis and Sintering of Translucent Yttrium Aluminium Garnet**" submitted by **Georgekutty Ulahannan (Roll No: 212CR2498)** in partial fulfilment of the requirement for the award of Master of Technology degree in Ceramic Engineering at **National Institute of Technology, Rourkela** is an authentic work carried out by his under my supervision and guidance. To the best of my knowledge, the matter embodied within this thesis has not been submitted to any other university/institute for the award of any other degree or diploma.

Dr. Debasish Sarkar

Dept. of Ceramic Engineering

National Institute of Technology

Rourkela- 769008

Acknowledgement

Fulfilment of this project and thesis would not have been conceivable without the help of numerous individuals, to whom I am extremely appreciative. As a matter of first importance, I would like to express my genuine appreciation to my supervisor Prof. Debasish Sarkar, Ceramic Engineering Department for his substantial sharing of wisdom, endless help, constant encouragement and never ending patience throughout the whole time of investigation. I would like to show my gratitude towards Prof. H. S. Maiti for his valuable suggestions during the on-session of my project work.

I might want to express my deepest appreciation and sincere respects to Prof. Santanu Bhattacharya, Prof. Swadesh Kumar Pratihar and Prof. Japesh Bera and other faculties for their constant motivation, support and guidance.

I would like to acknowledge certain institutions for allowing me to use the facilities namely: CGCRI-Kolkata for cold isostatic pressing, hot pressing and TEM, NIMS-Japan for Spark plasma sintering and ARCI-Hyderabad for Hot Isostatic pressing, respectively.

I am also thankful to staff and research scholars of Ceramic Engineering department especially Sangeeta Adhikari, Raju Mula, Sambi Reddy, Ashley Thomas, Prativa Adhikari, Jayarao Gorinta, for their support and help.

I am extremely indebted to my parents, my siblings and friends who always believed in me and gave all their support for all the decisions that I have made.

At last, I modestly bow my head with most extreme appreciation before the God Almighty who dependably demonstrated to me a way to go and without whom I couldn't have done any of these.

Georgekutty Ulahannan

Abstract

The prime objective of this investigation is the optimization of powder synthesis process and evaluation of their sintering behavior for futuristic laser host material. Selection of precursor and process variables for the large scale synthesis of yttrium aluminum garnet (YAG) nanopowder emphasizes in the first part of the dissertation. Co-precipitation of aluminum nitrate, yttrium nitrate and ammonium bicarbonate precursors below room temperature and their subsequent rapid calcination at 900^{o}C develops high crystalline, 40nm pure YAG nanoparticles in comparison with other six powder synthesis processes. Particles have near spherical morphology with consist of high surface area of 34m^2/gm. Batch size upto 250gm powder synthesis process has a high degree of reproducibility. Second part illustrates five different consolidation and sintering techniques of optimized YAG nanopowders known as uniaxial pressing – atmospheric sintering (UAS), cold isostatic pressing – atmospheric sintering (CAS), hot pressing (HP), uniaxial pressing – atmospheric sintering – hot isostatic pressing (UAS-HIP) and spark plasma sintering (SPS). Low degree of heating rate during conventional atmospheric sintering provides uniform equiaxed microstructure and better densification in presence of the optimum amount of silica content. Combination of UAS – HIP exhibits highest densification which is just above the spark plasma sintering process. Hot isostatic pressed disc (Ø ~15mm and thickness ~1.5mm) shows 99.6% relative density with average grain size of 2.5 micron. The transmittance of disc is around 60% in the visible region as well as near infra-red region of 550nm and 1100nm, respectively. This translucency behaviour is further needed to improve for laser host transparent ceramics.

Contents

List of figures

List of Tables:

CHAPTER 1

INTRODUCTION

1. Introduction

Yttrium aluminium garnet (YAG, having chemical formula $Y_3Al_5O_{12}$) is a significant host material for solid state laser and has recently become popular as a substrate material for optical components. Crystalline yttrium aluminum garnet has a cubic garnet structure. The YAG is a stable laser gain host compound, which is mechanically robust, physically hard, optically isotropic, and transparent from 300 nm to beyond 4 microns [1]. YAG single crystals are capable of receiving trivalent laser activator ions from both the transition and rare earth metal groups. It can be grown up with very low strain. YAG is not only a very significant laser material, but also a high-temperature structural material and a fluorescence material. Presently, Nd-doped YAG single crystal has been the most extensively used solid-state laser material applications.

Single crystals have been taking considerable attention since the early 1960s for fluorescence and solid-state lasers applications. However, more consideration has been paid to fabrication of the YAG ceramics since they have shown improved optical and high temperature mechanical properties [2]. Czochralski method is a common technique to produce single crystal YAG. In this technique, thecrystal is drawn out from a melt. Fabrication of YAG single crystals are highly expensive, and it is also difficult to make large size YAG single crystals. The gradual development during drawing of the crystal from the melt in a thermal gradient consequently has residual stress in a single crystal. The extremely stressed core with the stress pattern radiating outward may lead to the cracking either when cooling or during the period of operation. In single crystal, the level of active doping ions can be less accurate than preferred.

Processing of polycrystalline transparent ceramics has numerous advantages than conventional single crystal growth methods including faster production rate, possibility to

produce larger sizes and complex structures. Moreover, relatively large and uniform dopant concentrations and improved mechanical behavior can also be achieved. The temperature for sintering of transparent ceramics is lower than the melting temperature of the same. Therefore, it is easy to fabricate the polycrystalline transparent ceramics at lower temperatures compared to single crystals.The conditions [3] for the transparency of polycrystalline transparent ceramics are:

- The density of the sintered body should be very high (close enough to the theoretical density) and it should be free from pores.
- The sintered body should also be free from secondary phases such as inclusions, pores, intergranular films and composed of single phase.
- The grain size should be in sub-micron level if the crystallography of the structure is non-cubic.
- The band gap of the material should be higher than the energy of quanta of visible light.

The polycrystalline ceramic materials essentially consist of grains separated by the grain boundaries. These grain boundaries have a significant role in thermal and mechanical properties. Consequently, polycrystalline transparent ceramics has higher hardness and toughness compared to single crystal material. When an electromagnetic radiation falls on a transparent body, it experience reflection, refraction, absorption due to non-homogeneity and lastly gets transmitted over the other side of the sintered body. The grain boundary, inclusions, pores and rough surfaces are main scattering centres and cause of light absorption in a polycrystalline material. The different light scattering mechanisms has shown in the following figure [4].

(1) Grain boundary scattering

(2) Scattering due to pores or inclusions

(3) Scattering due to secondary phase

(4) Birefringence

(5) Surface scattering due to roughness

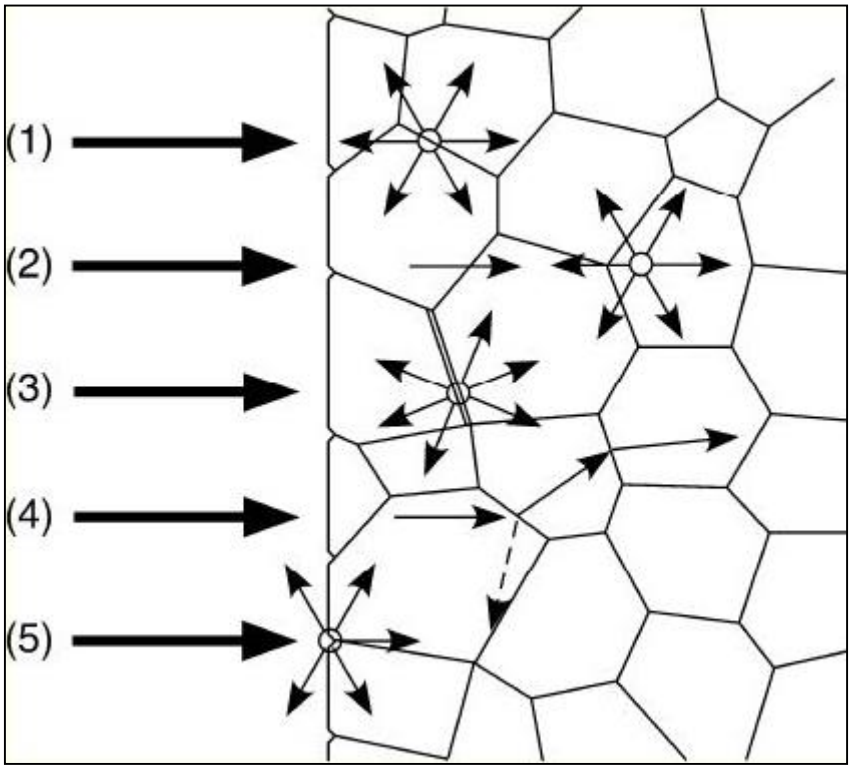

Figure 1.1 Different light scattering mechanisms in polycrystalline ceramics

There are three stable compounds at ambient pressure in the Y_2O_3- Al_2O_3 system apart from the end-member phases. These are $Y_3Al_5O_{12}$ (YAG), $YAlO_3$ (YAP) and $Y_2Al_4O_9$(YAM), respectively. The following phase diagram shows the different phases in the Y_2O_3 - Al_2O_3 system [5].

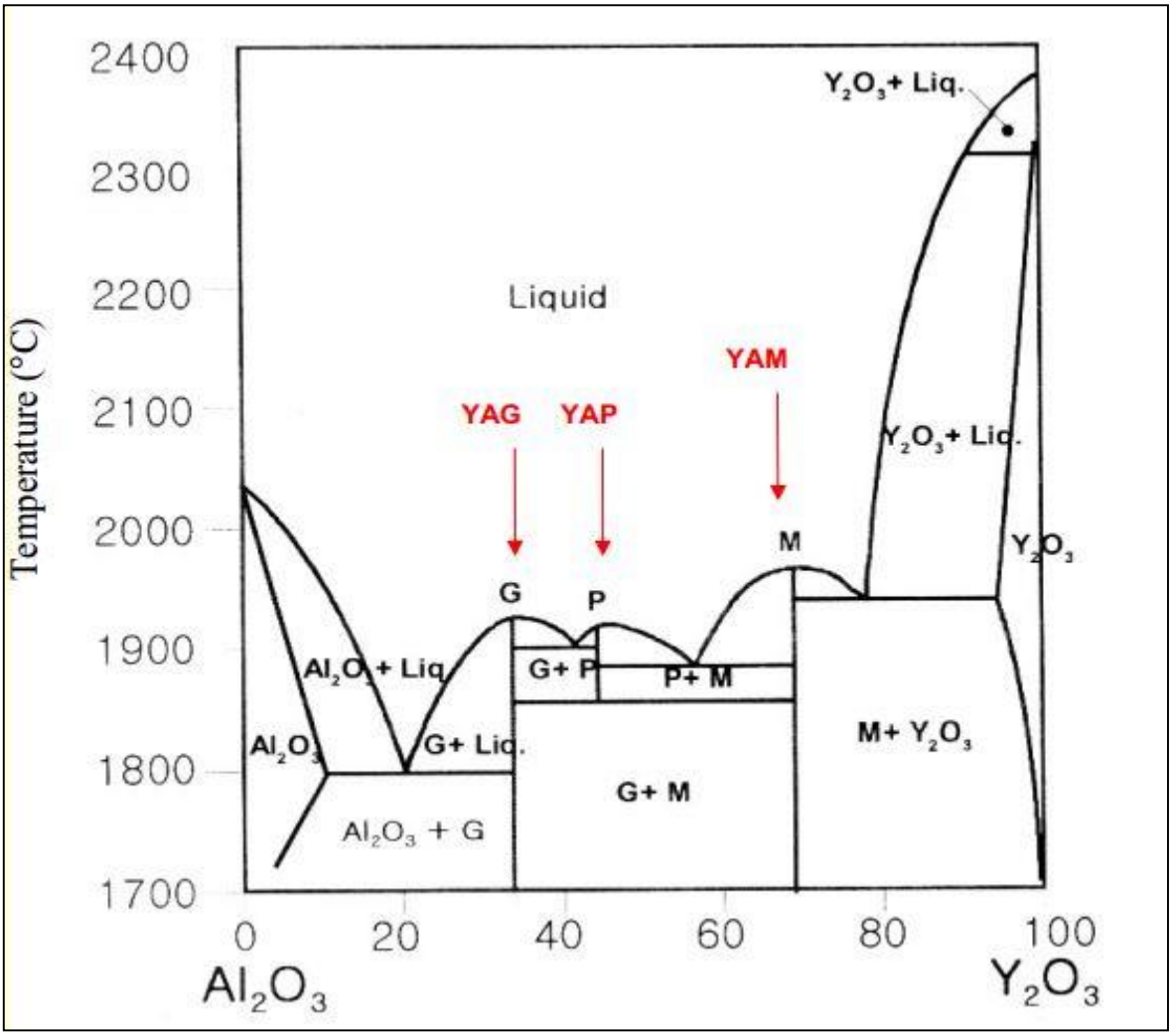

Figure 1.2 Yttria-alumina (Y_2O_3-Al_2O_3) phase diagram

Yttrium aluminium garnet (YAG - $Y_3Al_5O_{12}$) has a cubic crystal structure and both yttrium aluminium perovskite (YAP -$YAlO_3$), and yttrium aluminium monoclinic (YAM - $Y_2Al_4O_9$) has orthorhombic or hexagonal perovskite and monoclinic structures, respectively.

Yttrium aluminium garnet contains eight formulas per unit cell because of the cubic structure. The structure of garnet represents as $\{C_3\}[A_2](D_3)O_{12}$ where C, A and D represents the do-decahedral, octahedral and tetrahedral sites. The crystal structure of YAG [6] is shown in the following figure below;

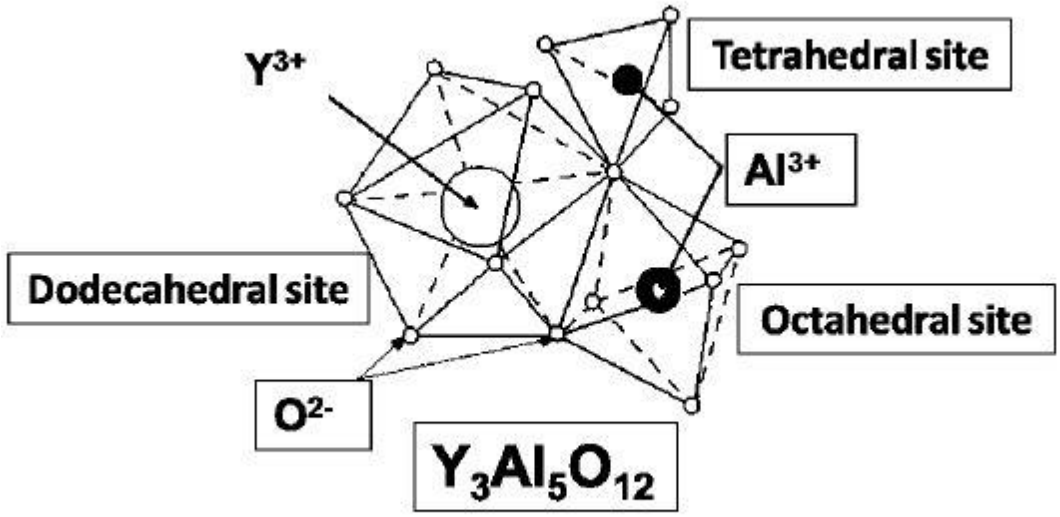

Figure 1.3 Crystal structure of YAG

The cationic ratio (Y:Al) of YAG is 3:5 so, a small deviation from the stoichiometry makes secondary phases such as YAM and YAP, respectively.

There are different kinds of methods that have been established to prepare YAG nanopowders and each method have different starting precursors, processing parameters, apparatus, etc. Earlier, YAG powder was conventionally produced by a solid state reaction between the component oxides which need frequent mechanical mixing and extensive thermal treatment. But the conventional solid state reaction has a problem of uncontrollable powder morphology. Various wet-chemical techniques have been established and effectively used in recent years for low-temperature preparation of phase-pure YAG nanopowders with a controllable morphology. These techniques include sol-gel processing [7-9], hydroxide co-precipitation [10-12], homogeneous precipitation [13], glycothermal treatment [14], spray pyrolysis [15-16], and combustion synthesis [17-19]. The sol-gel processing and co-precipitation are extensively used for powder synthesis. Fundamentally, the wet-chemical methods comprise of the procedure of extracting yttrium and aluminium ions instantaneously

from solution. The present work mainly focuses on the co-precipitation and sol-gel process for YAG nanopowder synthesis and optimization of the process has been done.

Commercially, the YAG transparent ceramics are prepared by different consolidation and sintering methods. The green compacts are made by using uniaxial pressing and cold isostatic pressing (CIP). Sometimes, the uniaxially pressed compacts are again consolidated by cold isostatic pressing for achievement of better green density. Achieving maximum green density will help to attain transparency after sintering. Tape casting and slip casting are also used for the consolidation purpose. Some consolidation techniques combine the application of pressure and temperature at the same time such as hot isostatic pressing (HIP), hot pressing (HP), spark plasma sintering (SPS), etc. The sintering of the YAG ceramics is difficult due to the high melting point. This high melting point (1930^{o}C) is due to the slow diffusion of yttrium ions that may be credited to the larger size of the same [20]. The sintering techniques are conventional sintering, vacuum sintering, etc. pre-sintering is done in some cases of HIP and hot pressing. Occasionally annealing is done after pressure assisted sintering processes to remove the residual stresses in the sintered body.

CHAPTER 2

LITERATURE REVIEW

2. LITERATURE REVIEW

2.1. Powder synthesis

The two important powder synthesis techniques of yttrium aluminium garnet are the solid state reaction process and wet chemical process. The wet chemical process is again classified into subsections which may include sol-gel processing, hydroxide co-precipitation, homogeneous precipitation and many more. The prime focus of the work is on powder synthesis processes with different methods and its optimization to prepare crystalline YAG nanopowder. Optimization of the sintering process has also been carried to achieve high density and transparency.

2.1.1 Solid state reaction

Chang-qing et al. [21] synthesized transparent polycrystalline YAG ceramics by solid-state reaction method using commercial ultrafine yttria and α-$A1_20_3$ powders. They milled the starting materials and calcined at 1400^{o}C, and sintered this powder at 1750^{o}C in a vacuum furnace for 4 hours to achieve YAG ceramics. They reported no reaction between Y_2O_3 and α-$A1_20_3$ phases in the as-milled powders. There are YAG, YAP, YAM, Y_2O_3 and α-$A1_20_3$ phases present in the calcined powder at 1300^{o}C and 1400^{o}C. The YAG powder was obtained after the 1500^{o}C calcination of the milled powders. The activity of 1500^{o}C calcined powder was not enough to produce transparency in the calcined product.

Tsai et al. [22] studied on the effect of the different aluminium sources on the formation of YAG powder via solid state process. They stated that the aluminium source for the formation of YAG powder is boehmite as compared to α-$A1_20_3$, θ-$A1_20_3$ and γ-$A1_20_3$. During the solid state reaction, the phase transformation of YAM→YAP→YAG was found. Diffusion of boehmite in the Y_2O_3 lattice destroys the powder shape of Y_2O_3. They prepared pure YAG

powder successfully by using boehmite as the aluminium source by calcining at 1500°C for 5h.

Kong et al. [23] applied mechanochemical solid state reaction process to prepare yttrium aluminium garnet (YAG) from Y_2O_3 and Al_2O_3 mixture. High energy ball milling significantly enhanced the reactivity of the mixed components. They achieved almost pure YAG phase after calcination at 1000°C for10 hours ball milled mixture with a particle size of 0.1μm - 0.2μm. They stated that this calcination temperature was lower than that required by conventional solid state reaction process. High energy ball milling of Y_2O_3 and Al_2O_3 enhances the density of the $Y_3Al_5O_{12}$ garnet.

Zhang et al. [24] conducted dry grinding of $Y_2O_3$and transition Al_2O_3 using a planetary ball mill to synthesize yttrium aluminum garnet (YAG). The mechanochemical reaction between Y_2O_3 and transition Al_2O_3 forms $YAlO_3$ and YAG after grinding for duration of 120 minutes. There was no reaction when $Al(OH)_3$ or α-$Al_2O_3$was ground with Y_2O_3. Grinding of yttria for 360 minute with transition alumina prepared by 400°C heating generates a nearly amorphous YAG phase. According to the reported data, the calcination of this amorphous YAG at 700°C gave a well crystallized YAG phase.

2.1.2. Co-precipitation process

Zhang et al. [25] prepared YAG powders by co-precipitation method in which NH_4HCO_3 was used as a precipitant and Y_2O_3 and $A1(NO_3)_3.9H_2O$ as raw materials. Two types of surfactant were added into the solution which are Polyethylene glycol (PEG10000) as steric stabilizer and $(NH_4)_2SO_4$ as an electrical stabilizer. They found that the presence of the PEG and $(NH_4)_2SO_4$was found favourable for making dispersion of the resulting YAG powder. The precursor had directly converted to pure YAG at about 900°C without any intermediates. The

YAG powder obtained from 1100^{o}C calcination for 2 hours was well dispersed, and the average particle size was ~78 nm.

Li et al. [26] synthesised Yttrium aluminium garnet (YAG) precursor via a co-precipitation method using ammonium hydrogen carbonate (AHC) as the precipitant and aluminium nitrate and yttrium nitrate as raw materials. The calcination of the precursor at 1200^{o}C gives fine and low-agglomerated YAG powder. A very few amount of YAM phase was found in the 1200^{o}C calcined powder. The particle size of the powder obtained from the above process is approximately equal to 120 nm and is very weakly agglomerated to a particle size of ~500 nm. They stated that the agglomerated particles had a porous structure with a netlike connection. This YAG nanopowder was sintered into transparent pellets by vacuum sintering at 1730^{o}C -1790^{o}C with 0.5 wt% of TEOS and 0.1 wt% of MgO additions.

Li et al. [27] in another study narrated two co-precipitation methods for the synthesis of YAG powder. They prepared YAG precursors by co-precipitation method of mixed solution of aluminum and yttrium nitrates using ammonia water and ammonium hydrogen carbonate as precipitants, respectively. They observed ammonium hydrogen carbonate surpasses ammonia water for the preparation of well-sinterable YAG powders. According to their study, the co-precipitation using ammonia water produced a gelatinous hydroxide precursor with an approximate composition of $Al(OH)_3.0.3[Y_2(OH)_5(NO_3).3H_2O]$. The 1000^{o}C calcination of precursor gave pure YAG phase via YAP intermediate phase. The sinterability of the YAG powder obtained from this process is poor because the particles are strongly agglomerated to each other.

The co-precipitation using ammonium hydrogen carbonate as precipitant gives a carbonate precursor of YAG having an approximate composition of $NH_4AlY_{0.6}(CO_3)_{1.9}(OH)_2.0.8H_2O$. 900^{o}C calcination directly gave pure YAG phase without any intermediate phase. The most

required calcination temperature for the carbonate precursor was determined as 1100^{o}C. This YAG powder has good dispersity and sinterability because of the less agglomeration of the dried precursor. The crystallite size of the particles obtained from 1100^{o}C is almost same, and it is approximately equal to 50nm. This YAG powder sintered to nearly full density by vacuum sintering at 1500^{o}C for 2 hours, and it showed translucency in the sintered product.

Marlot et al. [28] made YAG precursor by using consistent metal nitrates which was precipitated using ammonium hydrogen carbonate. They did calcination for one minute at various temperatures, the phases detected at 900^{o}C was YAP whereas complete conversion of YAG was possible at 1100^{o}C. The whole precipitation reaction was carried out at pH of 7.3, deviating from the pH of 7.3 produced secondary phases such as YAM and YAP. The pH was maintained constant all along the synthesis process in order to achieve pure YAG without intermediate phases. The obtained precursor was composed of aluminium and yttrium carbonates, ammonium and hydroxide. Precursor calcined at 1050^{o}C was pure nanopowder and the average grain size of the particle was 30nm.

Li et. al. [29] investigated the influence of aging and calcination temperature on the precursor composition and transformation temperature of yttrium aluminum garnet phase. They synthesised YAG powder by co-precipitation method with ammonium hydrogen carbonate as the precipitant. They observed that aging time has a dramatic effect on the precursor composition, which in turn influences the transformation temperature of the YAG phase. The precursor prepared without aging was loosely agglomerated, and 1000^{o}C calcination gives pure YAG phase with an average particle size of 50nm. This YAG powder particle had a spherical shape and good sinterability. The above powder was densified to good transparency by a TSS technique. The prepared precursor was severely agglomerated in appearance after 6h aging and required 1300^{o}C to achieve pure YAG phase.

Sang et al. [30] analysed the chemical evolution of YAG precursor by co-precipitation of yttria and aluminium nitrate dissolved in nitric acid and precipitated against ammonium bicarbonate. The precursors were prepared at different pH levels, and the effect of pH during the aging period was examined. It was noticed that a pH greater than 8.0 facilitated the formation of secondary phases such as YAP or yttria. A higher pH enabled re-dissolution of Al^{3+} cation hence disturbing the Y/Al ratio, which is essential for the synthesis of pure YAG. Preparation of pure YAG phase was possible at low pH with bi-carbonate precursors only rather than hydroxide precursors. Although the development of YAG was identified by an exothermic peak in DTA curve, but the temperature of 1300^{o}C for 3 hours was required for complete conversion of YAG phase.

Yang et al. [31] revised the process of co-precipitation by citric acid treatment. Use of citric acid empowers formation of YAG phase at 900^{o}C in addition to loosely agglomerated powder. These YAG powders were found highly dispersive in nature. There was a direct transformation of YAG phase rather than developing intermediate phases such as YAM and YAP. The reason for the reduced agglomeration was probably due to the association of cations with citric acid rather than water molecules.

Zheng et al. [32] produced YAG particles with a spherical morphology and particle size of 100 nm to 500 nm. The reaction medium was supercritical water where corresponding metal nitrate along with ammonium bicarbonate was used as starting a material followed by heating at 450^{o}C under high pressure for 4-6 hours in an autoclave. It was obtained that the particle size could be controlled by controlling the reaction time in supercritical water. This method did not introduce any organic impurities due to which the ceramic powder can be used successfully for the manufacture of transparent ceramics.

2.1.3. Sol-Gel Process

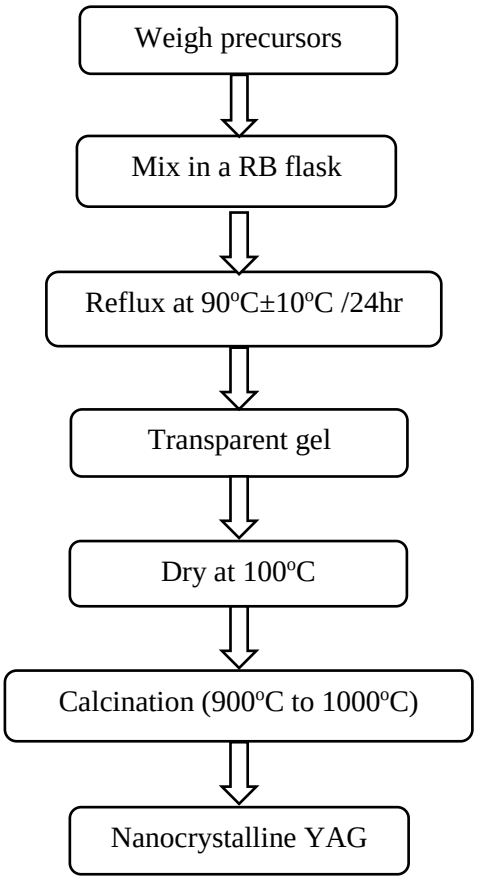

Figure 2.1 Sol-Gel Process flow chart [33]

Ramanujam et al. [33] synthesised nanocrystalline yttrium aluminium garnet (YAG) via sol-gel method using nitrate precursor. Stoichiometric aqueous solution of Y $(NO_3)_3.6H_2O$ and $Al(NO_3)_3.9H_2O$ was mixed in 1M citric acid solution. The schematic representation of sol-gel process is shown in Figure 2.1. The homogeneously mixed solution was immersed in thermostaticoilbathandrefluxedat90±10°C for 24 hours. The transparent gel like precursor was dried in the oven at 100°C for 24 hours. The 1000°C calcination of this transparent precursor for 1 hour gives nanocrystalline yttrium aluminium garnet. The particle size of the powder obtained from sol-gel process was ~30nm, and it has more agglomeration because of the complex networking of metal ions in the gel matrix.

Yang et al. [34] prepared Yttrium aluminum garnet (YAG) precursor by sol-gel combustion method using ethanol as solvent and aluminum nitrate, yttrium nitrate and citric acid monohydrate as starting materials. The stoichiometric solution was primarily heated at 60^{o}C and continuously stirred using a magnetic agitator for several hours until it turned to yellowish clear sol. Then it was stirred at 80^{o}C frequently, and the sol was converted into transparent sticky gel. The gel was quickly heated to 180◦C for 2 h, so that an auto-combustion reaction occurred and formed a xerogel, finally produced a yellowish fluffy precursor. The nano sized YAG powder obtained by precalcination of precursor at 500^{o}C and calcination at different temperatures. The powder begins to crystallize at 750^{o}C and 800^{o}C calcination gives pure YAG phase, moreover there is no intermediate phase like YAM or YAP. Precalcination reduced the crystallization temperature of YAG phase comparing with the process without precalcination. The particle size of the powder obtained from 900^{o}C calcination for 2 hours is measured as 30nm.

Sun et al. [35] explored a new sol-gel process for the preparation of yttrium aluminium garnet using aluminum-iso-propoxide and yttrium nitrate as starting materials with HNO_3 as catalyst. The homogeneous sol obtained from the reaction was dried in the oven at 40^{o}C, and the precursor was calcined at 850^{o}C to get pure YAG phase without any intermediate phase. The particle size obtained from the above process is around 20nm – 30nm.

2.2. Consolidation

In the fabrication of transparent ceramics, it is important to get a high green density and defect free green body before sintering. Attaining a density close to theoretical is only possible after only attaining of high compact green body through judicious ceramic processing technique. The different consolidation techniques implemented for preparing green bodies are uniaxial dry pressing, cold isostatic pressing (CIP), slip casting, gel casting

(thermal and non-thermal) and tape casting. In the present work, consolidation has been done by uniaxial pressing and cold isostatic pressing (CIP) of the calcined powders.

In uniaxial pressing, pressure is given in the uniaxial direction, so it results in a density gradient when the sample thickness increases. But in the case of CIP, uniform density is obtained because of hydrodynamic pressure. Li et al. [26] reported uniaxial pressing of powder followed by cold isostatic pressing (CIP). Uniaxial pressing was did for the shaping and consequent CIP for attaining a better green density. They pressed the powder uniaxially in a 20 mm die-mould at 10 MPa followed by cold isostatic pressing (CIP) at 250 MPa.

Slip casting is another consolidation technique used for ceramic body fabrication. Due to the homogeneous density and product volume, it is considered to be the best for the preparation of large shaped transparent ceramics. In slip casting process, the ceramic powder is dispersed in water by adding certain dispersing agent and preserving the pH to obtain the isoelectric point of a specific ceramic powder to avoid flocculation. The slurry is then casted into the porous plaster of paris mould, which draws the water content of the slurry and there by forming a ceramic body which can be considered as big hard agglomerate. Kwadwo et al. [36] prepared transparent YAG ceramics by slip casting. They used alumina and yttria powder as starting materials, poly(acrylic acid) as dispersant, polyethylene glycol added as a binder and citric acid used as a pH modifier.

Another fabrication process is tape casting in which ceramic slurry is assembled by doctor blading and stacking the individual tapes with different dopant concentrations. Tang et al. [37] reported the use of tape casting for the fabrication of optical grade YAG/Re:YAG/YAG (Re = Yb or Nd) composite laser ceramic. They used 4 wt% fish oil as dispersant to modify rheological behaviour of the slurry. In their work, polyvinyl butyral and butyl benzyl phthalate and poly-alkylene glycol were used as a binder and plasticizers, respectively.

Gel casting is another such method used for consolidation of ceramics. Herein, the ceramic powder is mixed with a monomer and homogenised in a slurry form. At a later stage cross linking polymer, catalyst and initiator are added to originate the polymerisation reaction after which a ceramic body is made, which has a high flexural strength as well as machinability to make perfect and desired shape of interest.

2.3. Sintering

Sintering is a processing technique used to produce materials with controlled density and microstructure by applying high temperature below its melting point. The main sintering techniques used for fabricating transparent ceramics are hot pressing, hot isostatic pressing (HIP), spark plasma sintering (SPS), vacuum sintering, and microwave sintering. It is also observed in the literature that vacuum sintering and hot isostatic pressing (HIP) are successfully used for the fabrication of transparent ceramics.

2.3.1. Pressureless Sintering

Yihua et al. [38] fabricated yttrium aluminum garnet (YAG) transparent ceramics by sintering at oxygen atmosphere. Tetraethyl orthosilicate (TEOS) was added as sintering additive, and it controls the grain growth and densification. The optimum amount of TEOS was 0.5 wt%. The samples were transparent after sintering at 1710^{o}C for 3 hours in the oxygen atmosphere and the grain size obtained was 4.95μm. The relative density of the compact was approximately equal to the theoretical density. At 1710^{o}C, the grain growth mechanism was solute drag and while at 1630^{o}C and 1550^{o}C the grain growth was controlled by liquid-phase-sintering mechanism. 80% transmittance at 1064nm was obtained in this sintered pellet.

Bhattacharyya et al. [39] highlights the role of silica on the densification behaviour of YAG in pressureless sintering. 2.5% fumed silica was used as an additive resulted into a more homogeneous and reactive intermediate. The YAG precursor powder was sintered at 1650ºC and the relative density obtained from above sintering was 93%. The solid solution formation was stimulated by silica phase through replacing Al^{3+} by Si^{4+}in tetrahedral site of YAG. This conversion leads to the development of Al^{3+}vacancies which improved the lattice diffusion coefficient and facilitated the YAG densification kinetics.

2.3.2. Hot Isostatic Pressing (HIP)

Suárez et al. [40] fabricated transparent YAG ceramics without aid of sintering additives by post- HIP from nano-sized precursor powder prepared using colloidal route. The cold isostatically pressed samples were sintered at 1650ºC and 1680º and then HIPed at 1650ºC and 1700ºC. The post-HIP process was done in an argon medium and the pressure of 200 MPa. The samples pre-sintered at 1650ºC reached a density of 99.7% by the HIP at both 1650ºC and 1700ºC. The HIPed samples showed pore free structure and mean grain size of 8μm. In HIP process, the main driving force for additional densification is mechanical stress applied by the pressurizing argon gas. A fair transmittance, upto 56% at 680 nm and near to 80% in the infrared range was obtained for this sample.

Zhang et al. [41] modified the optical properties of transparent YAG ceramics by post-annealing and post hot isostatic pressing. The isostatically pressed green body was sintered at 1780ºC for 20 hours in a high temperature vacuum sintering furnace under 10^{-3}Pa vacuum condition with a heating and cooling rate of 10ºC/minute. The sintered compact was air annealed at 1450ºC for 20 hours and post HIPed at 1700ºC for 2 hours under 200MPa of argon and then air re-annealed at 1250ºC for 10 hours. The above sintering technique gave pore free structure and mean grain size of 10μm. A decrease in oxygen vacancy

concentration after air annealing at 1450ºC was observed resulting in an increase of in-line transmittances of the samples. The post-HIP process at 1700ºC can decrease or contract residual intergranular pores in the sample. Re-annealing at 1250ºC removed oxygen vacancies induced by the HIP-treated samples but with re-annealing temperature increased, residual small intergranular pores made by the HIP-treated samples expanded and it resulted in the loss of transmittance. A high transmittance, upto 72% at 400 nm and 83% at 1064nm was obtained for this sample.

2.3.3. Spark Plasma Sintering (SPS)

Chaim et al. [42] made transparent polycrystalline YAG compacts using spark plasma sintering technique. They found an optimum condition for spark plasma sintering from various SPS conditions, such as heating at 1375ºC under 100MPa pressure for 3 minutes. This sintering condition gave a fast densification to achieve fully transparent material. The grain size obtained from this SPS condition was approximately equal to 500nm and relative density was more than 99%. At smaller SPS duration, when the grains are in the submicron size range densification might still be efficient by grain boundary sliding. On the other hand, at longer SPS durations the grains are in the micrometre range which upon further densification by grain boundary sliding is much difficult. This may result in residual pores, and an increase in residual pores size makes losses in transparency. The increase in the SPS pressure helps to achieve a density nearer to the theoretical density. This sintered disc has a transmittance of 32% at 900nm.

Frage et al. [43] prepared transparent YAG samples from 0.25 wt.% LiF doped nano sized YAG powder by spark plasma sintering (SPS) technique. Fully dense body was obtained after SPS process at 1300ºC under the pressure of 80MPa for a duration of 2 hours. They observed that presence of LiF plays an important role in the mass transport related effects throughout

the densification of YAG to full density and also in the removal of the residual carbon contamination. The average grain size obtained from the above process 1.7μm. 80% transmittance at infrared region was obtained in this sample.

Spina et al.[44] made fine grained yttrium aluminium garnet (YAG) ceramics by similar SPS process. A soft precursor obtained from co-precipitation of yttrium and aluminium chlorides solution was calcined to YAG powder. The sintered powder by SPS method at 1350ºC for 15 minutes and annealed at 800ºC for 1 hour in the air. The average grain size of the sintered body was 330nm, and with relative density of 99.99%. A transmittance of 66% at 600nm was obtained for this 1mm thick disc.

Frage et al. [45] investigated the effect of the spark plasma sintering (SPS) parameters and LiF doping on the mechanical properties and the transparency of polycrystalline Nd-YAG. The LiF additive affects mass transport, accelerates the densification and the grain growth in the progression of the SPS process. Hardness and bending strength are dropped in the presence of the LiF additive, in consistence with the increased grain size. The Young modulus is relatively unaffected by disparity of the processing parameters. They fabricated the sintered body by SPS at 1400ºC at 2ºC/minute heating rate and holding time 20 min. The optical transmittance in the LiF doped samples was higher as compared to the undoped ones. The improved optical transmittance of the doped samples, prepared in the carbon rich SPS environment was attribute to a possible cleansing effect of the fluorine component of the additive, which by merging with carbon forms volatile species that ejects as long as the open channels exist in the samples undergoing consolidation. 80% transmittance at wavelength 1000nm was obtained for this sample.

2.3.4. Vacuum Sintering

Liu et al. [46] made highly transparent YAG/1.0 at% Nd:YAG/YAG composite ceramic slab by vacuum reactive sintering method. The cold isostatically pressed compact was sintered at 1750ºC for 50 hours under vacuum of 10^{-5}Pa in the furnace equipped with tungsten mesh as a heating element. The sintered sample was annealed in air at 1450ºC for 20 hours to completely remove internal stress and remove oxygen vacancies. This sintered product was fully dense, and it had a mean grain size of 10μm. There was no pore and defects observed between or in the grains. The interface region among pure YAG and Nd:YAG showed an even microstructure, representing that there was no interface effect existing in the ceramic composite. The transmittance of the disc was 84% at 1064 nm.

Li et al. [47] discussed on the YAG ceramics preparation by two-step vacuum sintering. The isostatically pressed compact was sintered using two-step sintering process. The furnace first arises to 1800ºC with a heating rate of 10ºC/minute and then temperature rapidly decreased to 1680ºC and kept for 8 hours in a vacuum graphite tube furnace below 1.0 $\times 10^{-3}$Pa during holding process. In the first-step sintering, the grain size increases entirely because of coarsening. In the second-step sintering, the probability of densification without grain growth depends on the suppression of grain-boundary migration while keeping grain boundary diffusion active. The extended holding time was effective to promote further densification. The sintered samples has dense, pore free microstructure having a grain size of 7μm and has 84% transmittance in visible and near infrared region and 87% transmittance in mid-infrared region.

CHAPTER 3

OBJECTIVE

3. Objective

The objective of this project is synthesis and sintering of yttrium aluminium garnet for transparent ceramics.

- To optimize the powder synthesis process for the preparation of yttrium aluminium garnet (YAG) nanopowders from different powder synthesis techniques.
- To optimize the sintering technique to achieve high dense YAG from optimized YAG nanopowders.
- To study the optical transmittance of the sintered product.

CHAPTER 4

EXPERIMENTAL

4. Experimental Procedure

In this study, synthesis of YAG nanopowders was done by following seven different routes.

4.1. Powder synthesis process

Table 4.1 Different powder synthesis processes:

Process Number	Starting Materials	Process Identification	Precipitation Temperature	Temperature to achieve pure YAG
Process 1	$Al(NO_3)_3.9H_2O$, Y_2O_3,HNO_3 NH_4HCO_3	Co-precipitation by ammonium bicarbonate	7^oC	900^oC
Process 2	$Al(NO_3)_3.9H_2O$, $Y(NO_3)_3.6H_2O$ NH_4HCO_3	Co-precipitation by ammonium bicarbonate	7^oC	900^oC
Process 3	$Al(NO_3)_3.9H_2O$, $Y(NO_3)_3.6H_2O$ NH_4OH	Sol-Gel by ammonium hydroxide	7^oC	900^oC
Process 4	$Al(NO_3)_3.9H_2O$, $Y(NO_3)_3.6H_2O$	Direct precursor calcination	200^oC	1000^oC
Process 5	Al_2O_3, Y_2O_3	Solid state reaction	-	1100^oC
Process 6	$Al(NO_3)_3.9H_2O$, $Y(NO_3)_3.6H_2O$ NH_4HCO_3	Co-precipitation by ammonium bicarbonate	25^oC	950^oC
Process 7	$Al(NO_3)_3.9H_2O$, $Y(NO_3)_3.6H_2O$ NH_4OH	Sol-Gel by ammonium hydroxide	25^oC	950^oC

In the first process, synthesis of precursor was done by the addition of Aluminium Nitrate ($Al(NO_3)_3.9H_2O$), Y_2O_3 powder, NH_4HCO_3 and HNO_3. In the second process Aluminium

Nitrate ($Al(NO_3)_3.9H_2O$), Yttrium Nitrate ($Y(NO_3)_3.6H_2O$) and $NH_4HCO_3$was added. In the third process, Aluminium Nitrate ($Al(NO_3)_3.9H_2O$), Yttrium Nitrate ($Y(NO_3)_3.6H_2O$) and NH_4OH was added and in the fourth process direct calcination of Aluminium Nitrate ($Al(NO_3)_3.9H_2O$), Yttrium Nitrate ($Y(NO_3)_3.6H_2O$ was done. Direct solid state reaction was carried in the fifth process. Fifth and sixth process was similar to process second and third but carried at room temperature.

4.1.1. Co-precipitation of Aluminium Nitrate and Y_2O_3 using NH_4HCO_3 solution (Process 1)

Stoichiometric mixture of Aluminium Nitrate ($Al(NO_3)_3.9H_2O$), Y_2O_3 powder was added to distilled water and heated for 5 minutes followed by 2 drops of HNO_3 to the solution to clear the milkiness. The above solution was added to NH_4HCO_3 solution drop by drop, and this reaction was carried out in the ice bath at 10^oC. The pH value of the solution was kept constant at 7.3. After completion of the reaction, aging was done for 1 hr. The precipitate was separated by using a centrifuge at 5^oC and washed 2 times with distilled water. The precipitate was kept in the oven at 80^oC for drying and fine powder was obtained from grinding and sieving.

4.1.2. Co-precipitation of Aluminium Nitrate and Yttrium Nitrate using NH_4HCO_3 solution (Process 2)

Stoichiometric mixture of Aluminium Nitrate ($Al(NO_3)_3.9H_2O$) and Yttrium Nitrate ($Y(NO_3)_3.6H_2O$) was added to distilled water followed by stirring to get a clear solution. The above solution was added to NH_4HCO_3 solution dropwise. The reaction was carried out in ice bath. After the complete reaction, aging was done for 30 minutes and precipitate was separated by centrifuging at 5^oC and washed 2 times with distilled water. The grinding and sieving was done to the 80^oCoven dried powder to get a fine powder.

4.1.3. Co-precipitation of Aluminium Nitrate and Yttrium Nitrate using NH_4OH solution (Process 3)

The stoichiometric solution of Aluminium Nitrate ($Al(NO_3)_3.9H_2O$) and Yttrium Nitrate ($Y(NO_3)_3.6H_2O$) was prepared by mixing the above salts in distilled water followed by addition of NH_4OH solution in the ice bath. For the completion of the reaction, aging was done for 30 minutes. Similar isolation process was also adopted for precipitate as mentioned in the above process.

4.1.4. Direct precursor calcination (Process 4)

In direct precursor calcination, the stoichiometric mixture of Aluminium Nitrate ($Al(NO_3)_3.9H_2O$) and Yttrium Nitrate ($Y(NO_3)_3.6H_2O$) was added to 10 ml water and stirred well to get a clear solution. Then this solution was dried and calcined at 200^oC. The fine grinding of the powder was done for a further calcination at different temperatures to obtain the pure YAG phase.

4.1.5. Solid state reaction (Process 5)

In solid state reaction, stoichiometric mixture of Yttria (Y_2O_3) and Alumina (Al_2O_3) were mixed and ground the mixture in a mortar by using pestle. Dropwise addition of acetone was did for getting fine grounded powder. The paste like mixture was dried in oven at 70^oC for 2 hours. Different temperature calcination was done after powder preparation.

The processing temperature of the precursor will affect the characteristics of resultant YAG powder. Process 2 and process 3 are done in room temperature conditions to differentiate the results with low temperature process named as process 6 and 7, respectively.

4.2 Characterization of synthesized YAG powder

4.2.1. Thermal analysis

The phase transformation temperature and the decomposition behaviour of the precipitated powders were carried out by DSC-TG (NETZSCH STA 449C, Germany). In this instrument pair of thermocouple was attached to the sample and reference, respectively. The heat evolved or absorbed while the heating was measured by this thermocouple. The thermocouple produced small electric signals when the sample undergoes physical transformation because of seebeck effect and then the signals converted into heat evolved. It plots a graph of temperature vs. heat evolved curve having some peaks and dips. The peak and dip in the plot represented an exothermic and endothermic reaction resulting from evolution and absorption of heat, respectively. The powders were heated at a rate of 10^{o}C/min upto a temperature of 1200^{o}C.

4.2.2. X-Ray Diffraction analysis

Phase analyses of the calcined powders were executed by x-ray diffraction (XRD) using Cu Kα radiation in Phillips PANalytical (Model: PW 1830diffractometer, Netherland).The XRD arrangement was furnished with one-dimensional compound silicon strip detector for high quality diffraction data. The powder samples were placed on a non-diffracting sample holder positioned in the Bragg-Brentano diffractometer setup. The calcined powder obtained from different calcination temperature and different powder synthesis processes were analysed.

4.2.3. Surface area measurements by BET

Surface area measurement carried out by nitrogen multilayer adsorption of powder measured as a function of relative pressure using a fully automated analyser. The nitrogen follows at liquid nitrogen temperature and degassing was done at 200^{o}C for 3 hours. The amount of

adsorbed gas recovered measured the specific surface area of the sample. The obtained data was treated according to the adsorption isotherm equation. Surface area of different powders calcined at different temperatures measured with Quantachrome Nova Autosorb (Quantachrome instruments, USA).

$$\frac{1}{V_a\left(\frac{P_0}{P}-1\right)} = \frac{C-1}{V_m C} \times \frac{P}{P_0} + \frac{1}{V_m C}$$

Where,

P = partial vapour pressure of adsorbate gas in equilibrium with the surface at 77.4 K (b.p. of liquid nitrogen), in pascals

P_o = saturated pressure of adsorbate gas, in pascals

V_a = volume of gas adsorbed at standard temperature and pressure (STP) [273.15 K and atmospheric pressure (1.013×10^5 Pa)], in millilitres,

V_m = volume of gas adsorbed at STP to produce an apparent monolayer on the sample surface, in millilitres,

C = Dimensionless constant that is related to the enthalpy of adsorption of the adsorbate gas on the powder sample.

Then the BET value is given by following:

$$\frac{1}{V_a\left(\frac{P_0}{P}-1\right)}$$

The surface area is then calculated according to the equation:

$$S = \frac{V_m N_a}{m \times 22400}$$

where,

N = Avogadro constant (6.022×10^{23} mol^{-1}),

A = effective cross-sectional area of one adsorbate molecule, in square metres (0.162 nm^2 for nitrogen and 0.195 nm^2 for krypton),

M = mass of test powder, in grams,

22400 = Volume occupied by 1 mole of the adsorbate gas at STP allowing for minor departures from the ideal, in millilitres.

The specific surface areas of the powder obtained from different processes are measured using Quantachrome Nova Autosorb (Quantachrome instruments, USA) and values were tabulated in results and discussion.

4.2.4. Particle Size Analysis

The particle size of the powder can be calculated on putting the BET surface area value to the equation: $D = {}^{6}/_{\rho S}$

Where,

D = diameter of the particle

ρ = density of particle

S = surface area of the measured by BET

4.2.5. Morphological analysis by Transmission Electron Microscopy (TEM)

The morphological analyses of calcined YAG powder obtained from different processes were determined by Transmission Electron Microscopy (TEM). A highly accelerated electron beam generated by a potential drop of 120 KV was used in TEM. This electron beam passes

through the sample and some of them were scattered. The electrons were detected by an electron sensitive screen in the instrument setup and this will convert into an image.

4.3. Compaction

Table 4.2 Different consolidation techniques:

Process	Consolidation/Sintering
S 1	Uniaxial Pressing → atmospheric sintering in muffle furnace
S 2	Cold Isostatic Pressing → atmospheric sintering in muffle furnace
S 3	Hot Pressing (HP)
S 4	Spark Plasma Sintering (SPS)
S 5	Uniaxial Pressing → atmospheric sintering in muffle furnace → Hot Isostatic Pressing (HIP)

The YAG powder obtained from the process 2 was used to prepare the pellets. The powder was passed through a sieve having 150 mesh sizes for obtaining uniform particle size with better flowability. So compaction of this powder gives better green density. The important process parameters of the pellet preparation are addition of the binder, sintering additive, type of compaction, heating rate and the type of sintering. The pellets are made with and without binder addition where poly vinyl alcohol (PVA) was used as binder. Different batches of pellets were made with and without SiO_2 as sintering additive. The SiO_2 weight percentage was different in different batches that were 0wt%, 0.15wt%, 0.25wt% and 0.3wt%.

4.3.1. Uniaxial pressing

The different batches of powder were filled into a circular die made with carbon steel and uniaxially pressed at around 110MPa. The dwell time for pressing was 120 seconds. The punch was applied uniaxially to the powders within a confined space of die. During pressing of loose ceramic powders, there were three steps that were classified into the stages of compaction as rearrangement, deformation and fragmentation.

4.3.2. Cold isostatic pressing (CIP)

Cold isostatic pressing applied pressure from multiple directions for achieving greater uniformity of compaction and increased shape capability, compared to uniaxial pressing. The powder was encased in a rubber sheath that was immersed in a liquid which transmits the pressure uniformly to the powder. The pellets were prepared by applying a load of 275 MPa.

4.4. Sintering of Compacts

Sintering is a processing technique to produce materials with controlled density and microstructure by subjecting the pre-consolidated green body to higher temperature below its melting point. The driving force for sintering is the reduction in the free energy of the system. Both densification and coarsening result is a reduction in free energy of the system. Sintering is a competitive process of grain growth and densification.

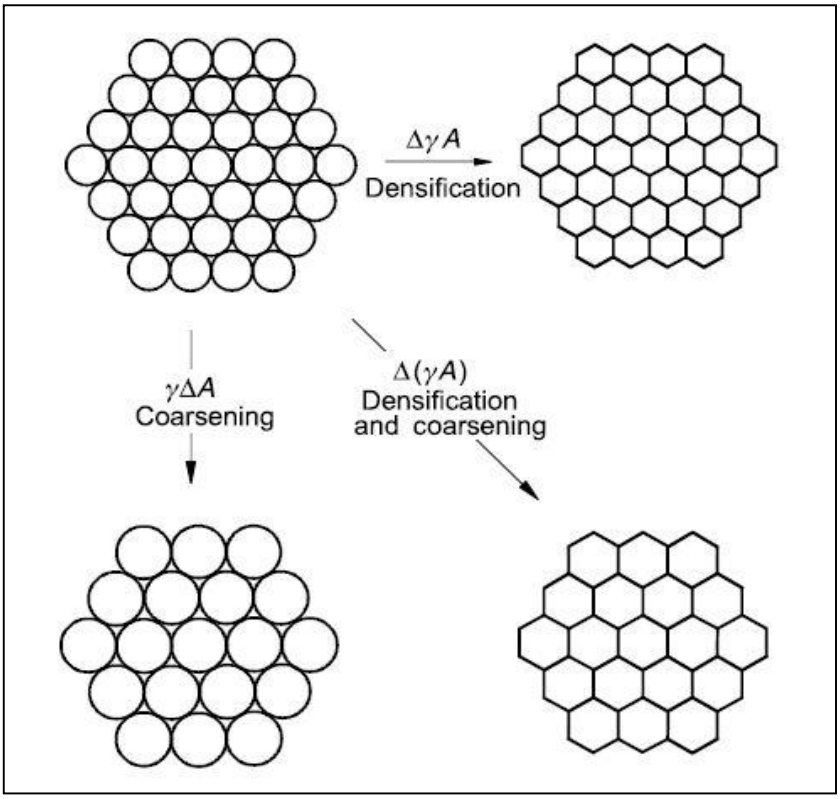

Figure 4.5 Schematic of different phenomena occurring through sintering

The pores in the body causes scattering of incident light, therefore achieving the transparency, the sintered compact should attain a very high density. And it should have uniform smaller grains for better mechanical properties like strength, thermal shock resistance, etc. A variety of sintering process are used for the preparation of transparent ceramics such as conventional sintering, hot pressing (HP), hot isostatic pressing (HIP), spark plasma sintering (SPS), etc.

4.4.1. Conventional sintering

The conventional sintering makes use of longer duration of dwell time at the final temperature for the elimination of residual porosity and often results in non-uniform grain growth. The heating rate was constant until it reaches the peak sintering temperature. Different heating rate and sintering temperature were used for the sintering process. The sintering was carried out by using a PID (Libratherm) controlled lab furnace.

Table 4.3 Different conventional sintering schedule and parameters:

Sample Name	Method of Compaction	SiO_2Amt (wt%)	Heating Rate (^oC/min)	Soaking Time and Temperature
YAG 1	Uniaxial	0.5	4	1700^{o}C/1hr & 1650^{o}C/8hr
YAG 2	Uniaxial	0.5	8	1700^{o}C/2hr & 1650^{o}C/8hr
YAG 3	Uniaxial	0.5	2	1700^{o}C/2hr & 1650^{o}C/8hr
YAG 4	Uniaxial	0.5	2	1650^{o}C/8hr & 1700^{o}C/2hr
YAG 5	CIP	0.5	2	1650^{o}C/8hr, 1700^{o}C/2hr & 1500^{o}C/5hr
YAG 6	Uniaxial	0.5	2	1650^{o}C/4hr &1550^{o}C/15hr
YAG 7	CIP	0.5	2	1650^{o}C/4hr &1550^{o}C/15hr
YAG 8	Uniaxial	0.5	2	1600^{o}C/4hr &1500^{o}C/16hr
YAG 9	CIP	0.5	2	1600^{o}C/4hr &1500^{o}C/16hr
YAG 10	Uniaxial	0.5	2	1400^{o}C/16hr &1600^{o}C/5min
YAG 11	CIP	0.5	2	1400^{o}C/16hr &1600^{o}C/5min
YAG 12	Uniaxial	0	2	1700^{o}C/30min
YAG 13	Uniaxial	0.15	2	1700^{o}C/30min
YAG 14	Uniaxial	0.3	2	1700^{o}C/30min

4.4.2. Hot pressing

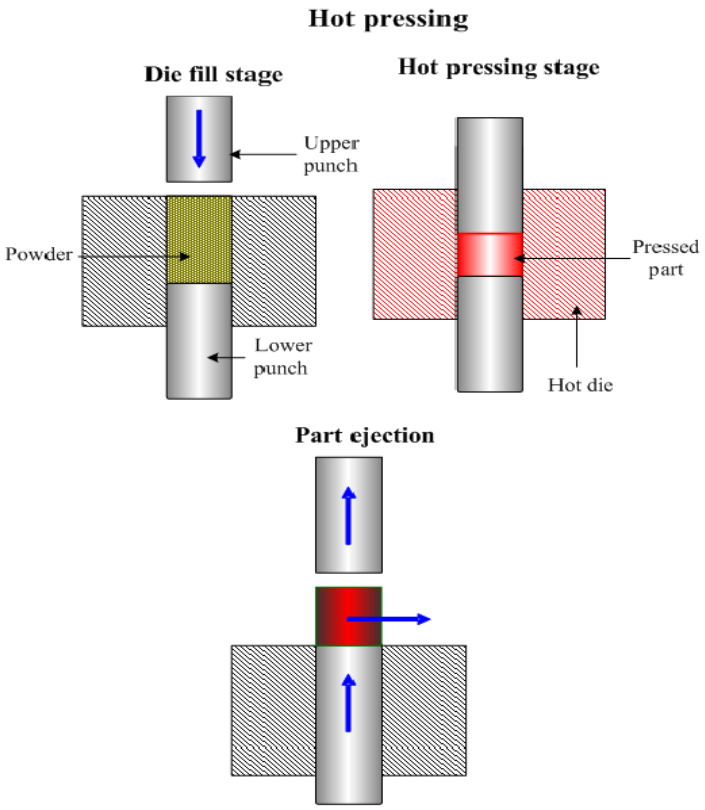

Figure 4.6 Schematic representations of different stages during Hot Pressing

The pre-compacted part was filled in a mould and it was heated to 1800^{o}C with a heating rate of 10^{o}C/min. The mould was made out of graphite and placed in an induction coil. When it was subjected to a high frequency electromagnetic field, the mould gets heated by induction. A uniaxial pressure of 35 MPa was applied at 1500^{o}C. The hot pressed compact was annealed at 1500^{o}C for 8 hours after hot pressing to eliminate the stress. Hereafter, hot pressed pellet is labelled as YAG 15.

4.4.3. Spark Plasma Sintering (SPS)

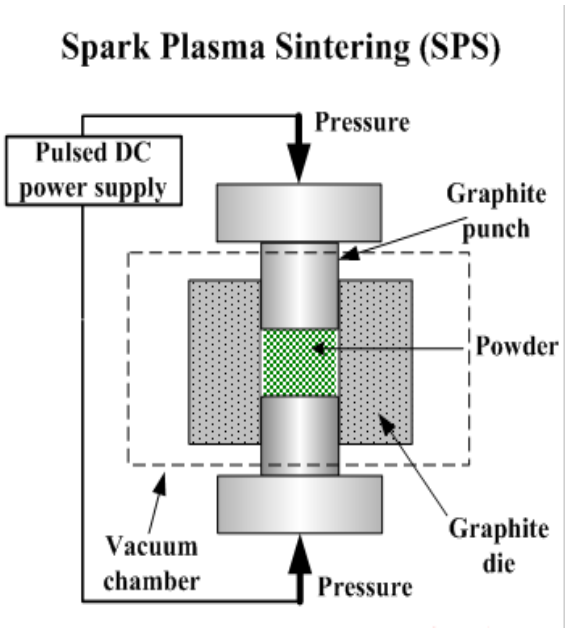

Figure 4.7 Schematic representation of Spark Plasma Sintering (SPS)

Spark plasma sintering follows the pulsed electrical current and pressure on the sample with comparatively less time to complete the sintering process at relatively low temperature [48]. This high sintering rate is possible in SPS, since high heating rates can be easily attained due to internal heating of the sample as opposed to external heating as seen in case of conventional sintering. Herein, sintering time reduces due to small holding time at sintering temperature. In SPS, very high heating rates (~ 500°C/min) can be achieved by the application of pulsed electrical current and pressure, simultaneously. A pulsed direct current passes through an electrically conducting pressing die working as the heating element giving more rapid densification rate due to the use of pressure and rapid heating rate. The presence of a pulsed electrical field might create sparks during the initial part of the sintering, which cleans the particle surface and facilitates grain boundary diffusion. Electrical field induced diffusion processes might also contribute to increased densification rate. The powder was sintered at 1300^{o}Cunder 60MPa. Hereafter, SPS pellet is labelled as YAG 16.

4.4.4. Hot isostatic pressing (HIP)

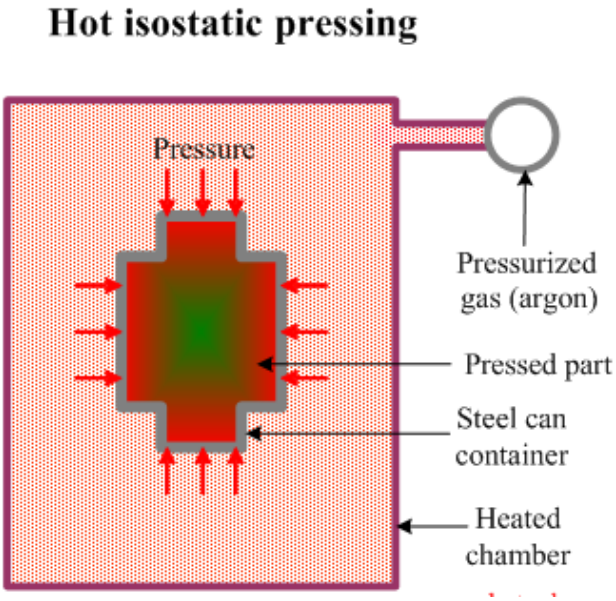

Figure 4.8 Schematic representation of Hot Isostatic Pressing (HIP)

Hot isostatic pressing subjects a component to both higher temperature and isostatic gas pressure in a controlled high pressure containment vessel. The uniaxial pressed followed by atmospheric sintered disc was filled in a container and followed the temperature increment of 1800^{o}C with an isostatic pressure of 195MPa by pumping argon gas to the chamber. Hereafter, HIPed pellet is labelled as YAG 17.

4.5. Characterization of compacts

4.5.1. Density characterisation

The bulk density and apparent porosity of the pellets made by different sintering processes was measured using Archimedes principle and the values are given in the following table.

Table 4.4 Density measurement of sintered samples:

Sample Name	Bulk Density (g/cc)	Relative Density (%)	Apparent Porosity (%)	Grain size (µm)
YAG 1	4.43	97.36	1.60	2.14
YAG 2	4.41	96.98	0.24	2.17
YAG 3	4.39	96.48	0.63	2.73
YAG 4	4.42	97.20	0.80	3.05
YAG 5	4.44	97.76	0.47	3.2
YAG 6	4.11	90.52	1.70	3.09
YAG 7	4.10	90.30	0.72	3.19
YAG 8	4.20	92.37	1.76	4.90
YAG 9	4.25	93.58	1.16	3.71
YAG 10	4.32	95.09	1.81	2.27
YAG 11	4.36	96.00	1.05	2.73
YAG 12	4.36	95.91	0.45	2.29
YAG 13	4.39	96.54	0.30	1.59
YAG 14	4.39	96.54	0.15	2.16
YAG 15	4.24	93.29	1.88	6.02
YAG 16	4.51	99.15	1.13	Grain boundary is not visible
YAG 17	4.53	99.63	0.42	2.50

4.5.2. Microstructure analysis

The microstructures of the sintered sample were viewed under Field Emission Scanning Electron Microscope (FEI Nova NanoSEM450) system. The electron gun having a field-

emission cathode delivers narrower probing beams at low as well as high electron energy, bringing about both enhanced spatial resolution and minimized sample charging and damage. FESEM imaging was done at different magnifications to the pellets.

4.5.3. Transparency measurement of HIP sample

The well-polished hot isostatically pressed sample was analysed in a UV-VIS spectrophotometer to determine the transmission percentage. The transmittance was measured for a range of 350nm to 1100nm wavelength, whereas the visible wave length is from 400nm to 700nm and near-infrared region is from 700-1100nm. The transmission behaviour was considered of visible wavelength at 550nm.

CHAPTER 5

RESULT AND DISCUSSION

5. Results and Discussions

5.1. Thermal analysis of the precursors

Initially, we have carried the thermogravimetric-differential thermal analysis (TG-DTA) to understand the mass loss at different temperatures and also the phase transformation phenomena.

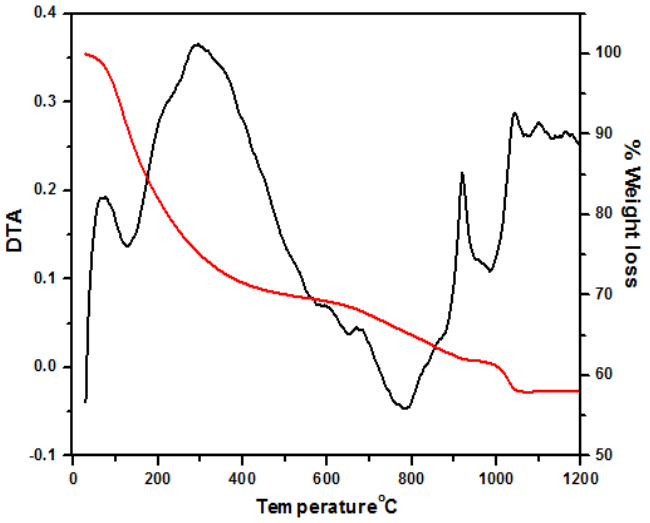

Figure 5.1TG-DTA for YAG precursors of Process-1

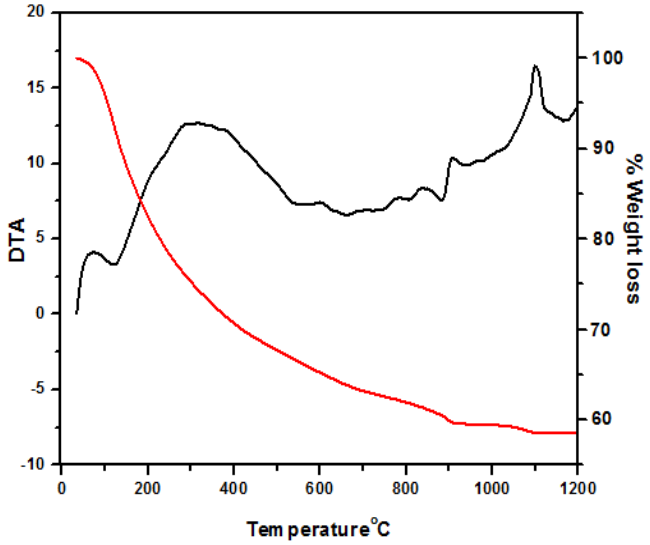

Figure 5.2 TG-DTA for YAG precursors of Process-2

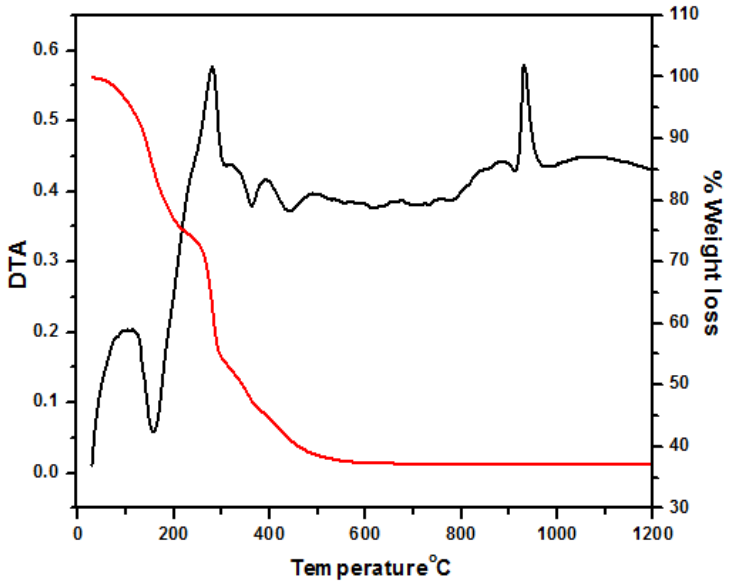

Figure 5.3 TG-DTA for YAG precursors of Process-3

Figure 5.1 represents the thermal analysis of precursor obtained by process 1. The endothermic peaks at around 100^{o}C attributes to the evaporation of physically absorbed water. That peak ranging from 200^{o}C to 400^{o}C corresponds to the decomposition of nitrate and chemically absorbed water. The sharp peaks at 920^{o}C and 1050^{o}C corresponds to formation of YAP and YAG phase, respectively. The mass loss due to the heating is around ~42%.

Figure5.2 represents the thermal analysis of precursor from process 2. We can observe that at around 100^{o}C desorption of physically bonded water takes place. The broad exothermic hump like peak between 200^{o}C to 400^{o}C corresponds to the decomposition of ammonium nitrate, crystalline water and partial decomposition of carbonates present in the precursor. The peaks in the range of 600^{o}C to 800^{o}C correspond to the decomposition of carbonates. A small exothermic peak at 925^{o}C represents the crystallization of YAG phase. There is a weight loss of ~39% observed due to the heating.

Thermo-gravimetric analysis of process-3 precursor is shown in Figure 5.3. Similar decomposition is observed at around 100^{o}C for physically absorbed water. A mass loss of 25% is observed till 230^{o}C. It can be seen that a total of 63% mass loss occurs due to heating. The sharp peak at 931^{o}C corresponds to YAG phase transformation.

5.2. XRD Analysis

The room temperature powder XRD pattern is obtained to understand the crystallinity and phase. Figure 5.4shows the XRD patterns of the process-1 precursor and precursor calcined at different temperatures i.e., 600^{o}C, 750^{o}C, 800^{o}C, 850^{o}C and 900^{o}C, respectively. The initial precursor and calcined precursor at 600^{o}C shows amorphous nature of the powders. No obvious diffraction peaks observes for this particles. Initialization of YAG crystalline phase formation is seen at 750^{o}C. The XRD pattern shows that the diffraction peaks became stronger and sharper with the increase in calcination temperature. A well crystallized YAG phase is observed for temperature above 800^{o}C. The phase remains constant till 900^{o}C.

Figure 5.5 represents the XRD pattern of calcined precursors at different temperatures from process-2. A low crystalline YAG phase is obtained at 750^{o}C. At 800^{o}C and 850^{o}C, YAP phase is seen which diminishes at 900^{o}C. The calcined powder at 900^{o}C gives perfect diffraction peaks for YAG phase with high crystallinity as observed in process-1. On comparing the crystallinity, YAG powders obtained by process-2 at 900^{o}C has high crystallinity than process-1 YAG powders.

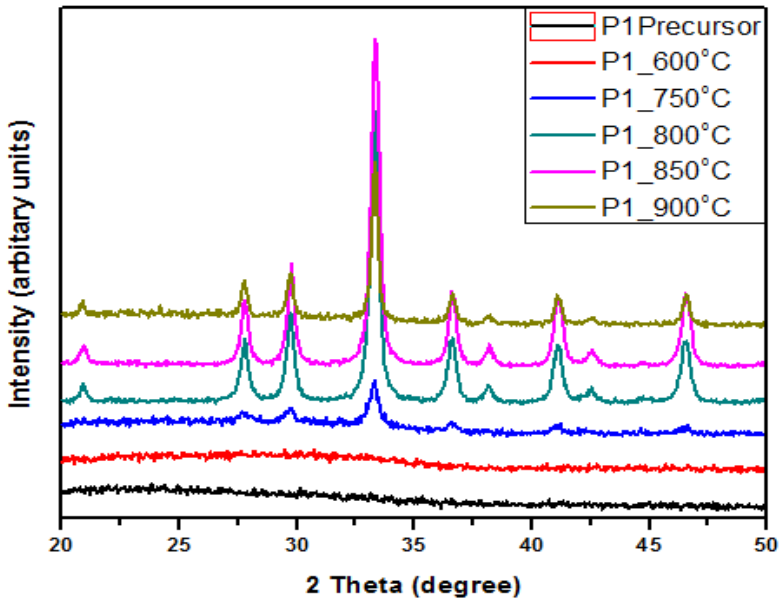

Figure 5.4Composite XRD patterns of YAG nanopowders following Process-1

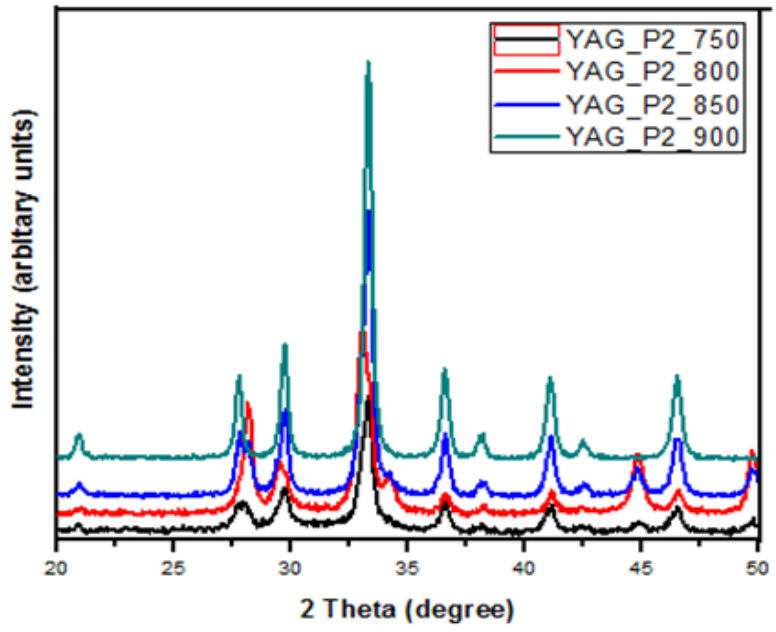

Figure 5.5 Composite XRD pattern of YAG nanopowders following Process-2

From the above processes we have observed that 750°C is the initialization temperature for YAG phase and 900°C is the optimum temperature for pure YAG crystalline phase. Figure 5.6 shows the XRD pattern of process-3 powders calcined at 750°C and 900°C, respectively. For this process, there was no obvious diffraction peaks obtained for powder calcined at 750°C which depicts amorphous nature of the powders. The powders calcined at 900°C shows perfect diffraction peaks free from other phases or impurities. In process-4, the direct calcination of Aluminium Nitrate ($Al(NO_3)_3.9H_2O$) and Yttrium Nitrate ($Y(NO_3)_3.6H_2O$) gives YAG phase at 900°C as shown in Figure 5.7. In the case of process-5, solid state reaction of the precursor does not give pure YAG phase at 900°C as shown in Figure 5.8. It reveals that, it requires a higher temperature for transformation to pure YAG phase.

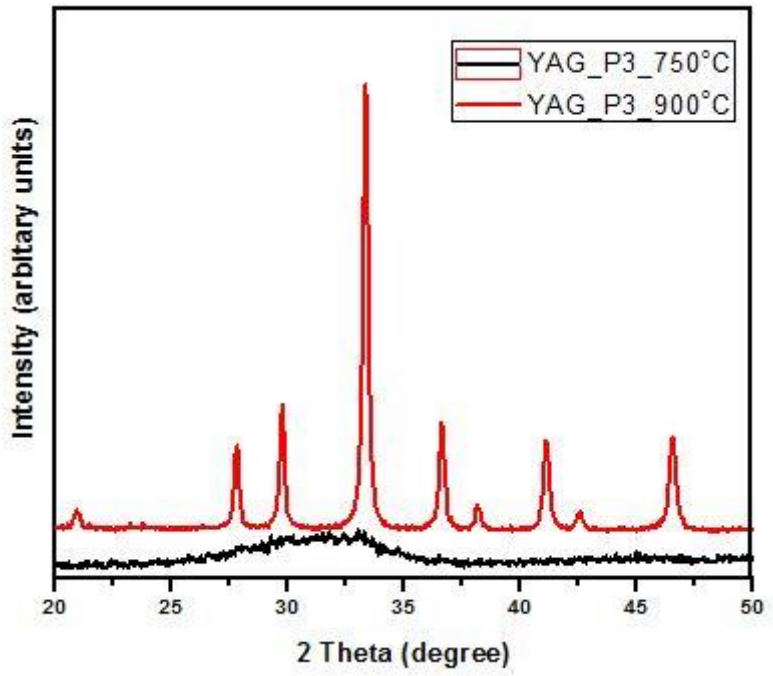

Figure 5.6 Composite XRD pattern of YAG nanopowders following Process-3

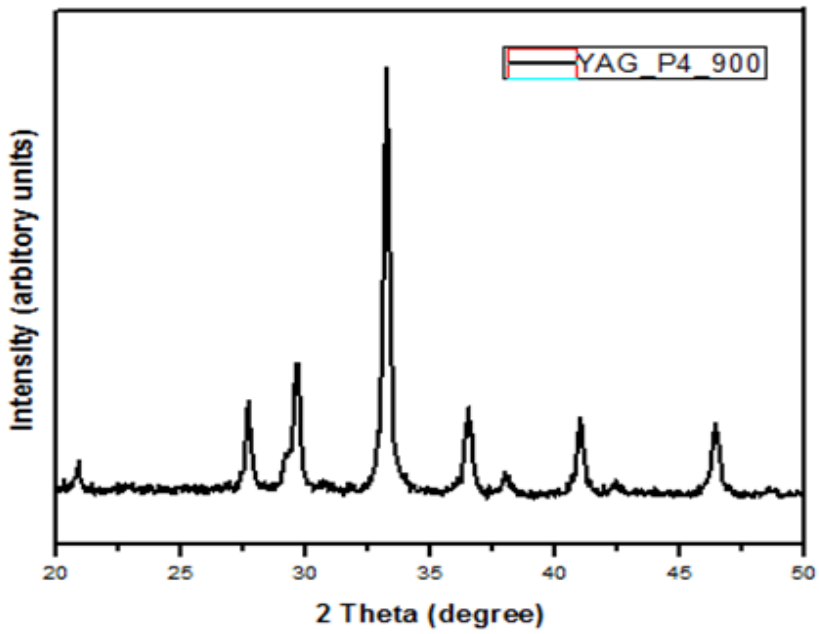

Figure 5.7 XRD pattern of YAG nanopowders following Process-4

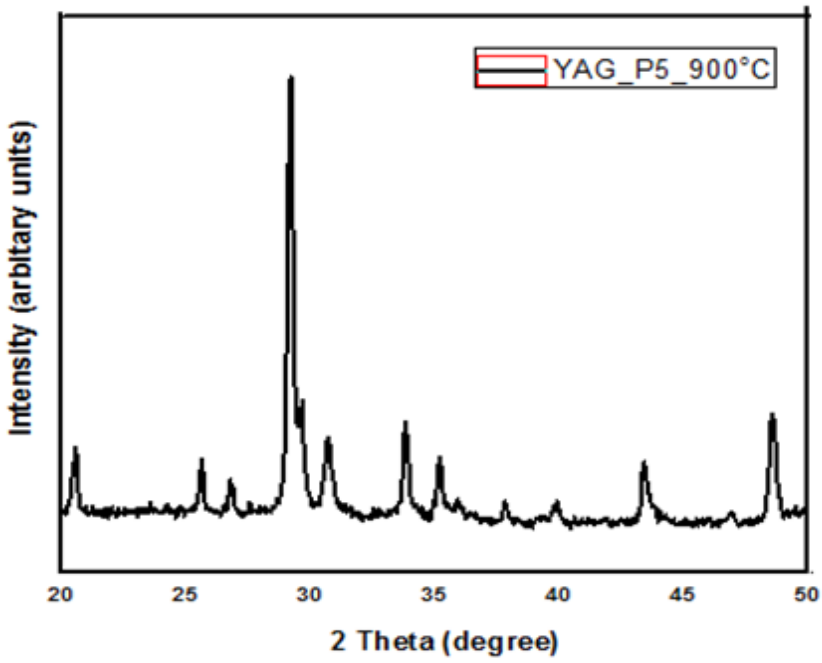

Figure 5.8 XRD pattern of YAG nanopowders following Process 5

The processing temperature of the precursor critically affects the characteristics of resultant YAG powder. In all the experiments till process-3, precursors are prepared below 10^{o}C. A repetition of process-2 and 3 is carried at room temperature to understand the difference in crystallinity and phase transformation namely process-6 and 7, respectively. Figure 5.9shows the XRD pattern of 900^{o}C calcined powders from process-2, process-6 and process-7. The calcined powders at 900^{o}C from process-6 and 7 shows pure YAG crystalline phase. The calcined powders from process-2 are observed to have high crystallinity among the three processes. Based on the morphological analysis, particle size and surface area as discussed in later section, calcination of process-2 precursor at 900^{o}C has been optimized to give pure YAG crystalline phase. Although, process-1 and 2 has near to equal surface area but the reproducibility of the process-1 was difficult and yield was comparatively less. Therefore, process-2 was chosen as the optimized process. The XRD pattern of the YAG powder obtained from process-2 calcined powder at 900^{o}C is shown in Figure 5.10.

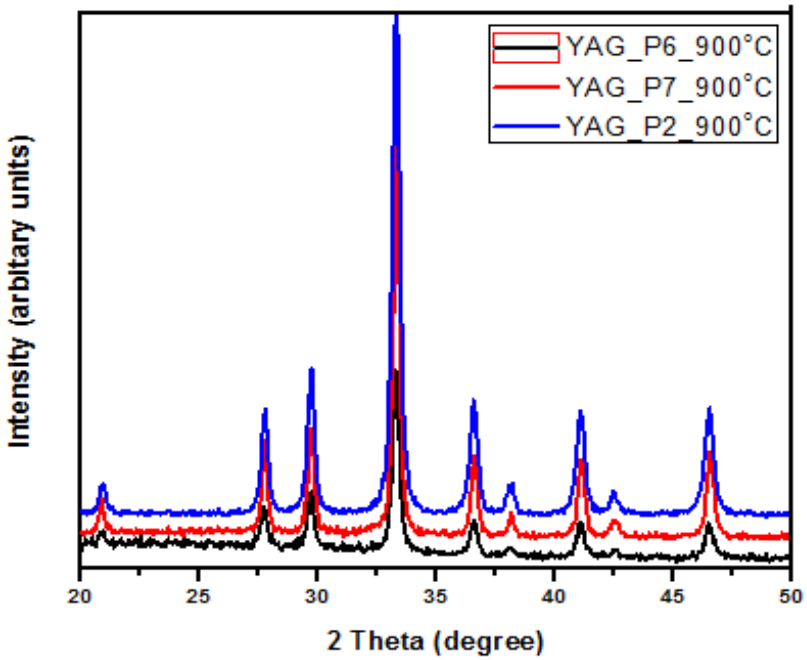

Figure 5.9 Composite XRD pattern of YAG nanopowders for P6, P7 and P2.

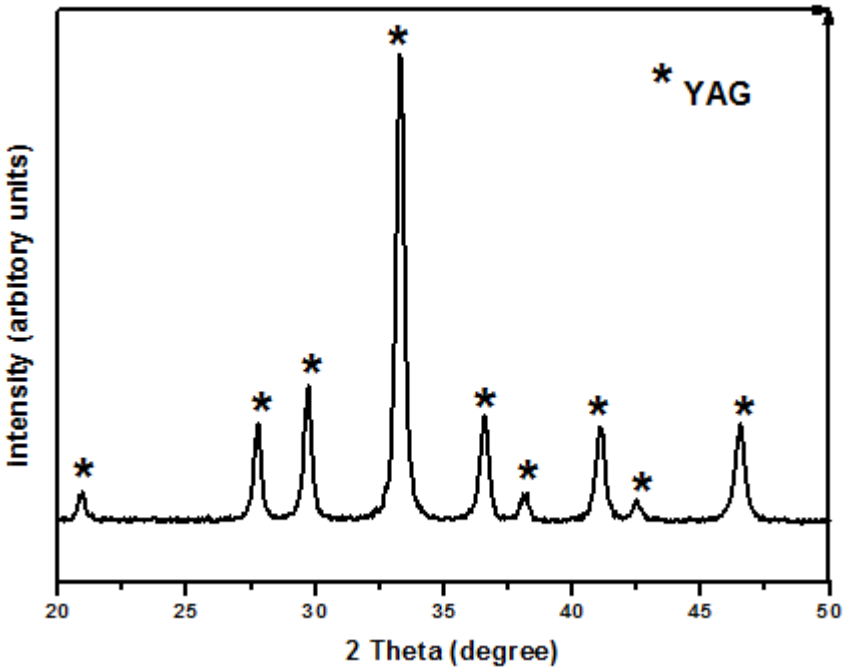

Figure 5.10 XRD pattern of P2 powder calcined at 900ºC (optimized powder)

5.3. Surface area measurement of powders obtained from different process

The surface areas of the powders calcined at different temperatures are analysed using BET surface area measurement. The highest surface area achieved is 33.69m^2/gm for the powder obtained from process-2. The powder prepared using process-1 also gives a surface area close to the highest value but the process has been eliminated due to reproducibility and yield. Powders obtained from co-precipitation gives more surface area because of the small particle size of powder and low calcination temperature compared to solid state reaction and direct precursor calcination processes. High surface activity is observed for powders having high surface area that requires less surface energy. The lowest surface area of ~5.25m^2/gm is obtained for the solid state reaction process. This reduction in surface area is caused by the increased particle size due to solid state process and high temperature calcination.

Table 5.5 Surface area of powders obtained from different processes:

Process	Process 1	Process 2	Process 3	Process 4	Process 5	Process 6	Process 7
Surface area (m^2/gm)	33.27	33.69	32.13	9.26	5.25	26.27	25.39

5.4. Particle size of powders obtained from different processes

The particle sizes of the powders obtained from co-precipitation synthesis are similar. In comparison to the other processes, the particle obtained from co-precipitation process has smallest particle size. Table 5.6 represents the comparative particle sizes of all the processes. An average particle size of 40nm was obtained from BET analysis for process-1 and 2. The solid state reaction in process-5 gives the highest particle size value ~260 nm compared to the co-precipitation process. Particle size of the calcined YAG powder is affected by powder synthesis process parameters like processing and calcination temperature. From this study, it is clearly shown that the co-precipitation process gives the smallest particle size and low temperature synthesis and calcination prevents the increment in the particle size. Particle size affects the packing of particles in green compacts and it also affects the grain sizes after sintering of the material. From the above results, it is clear that co-precipitation method in process-2 is the best method to obtain highly crystalline YAG powder with low particle size.

Table 5.6 Particle size of powders obtained from different processes:

Process	Process 1	Process 2	Process 3	Process 4	Process 5	Process 6	Process 7
Particle Size (nm)	40	40	41	150	260	50	55

5.5. Powder morphology analysis

The TEM image of the YAG nanopowder from optimized process-2 has been shown in Figure 5.11.We can observe that these powders have nearly spherical morphology and they are loosely agglomerated to form secondary particles. The average particle size as found from TEM image is ~42nm. It is also clearly seen that the particles are well dispersed. Spherical particles help in better packing of particles in the time of compaction to enhance the densification of the compact. Compared to the powders obtained from hydroxide precursor, carbonate precursors gives less agglomerated powders. Extreme agglomeration of the particles obtained from hydroxide precursor is essentially because of the bridging of nearby particles with water by hydrogen bonding. On the other hand, in carbonate precursor the possibility of formation of hydrogen bond is significantly reduced.

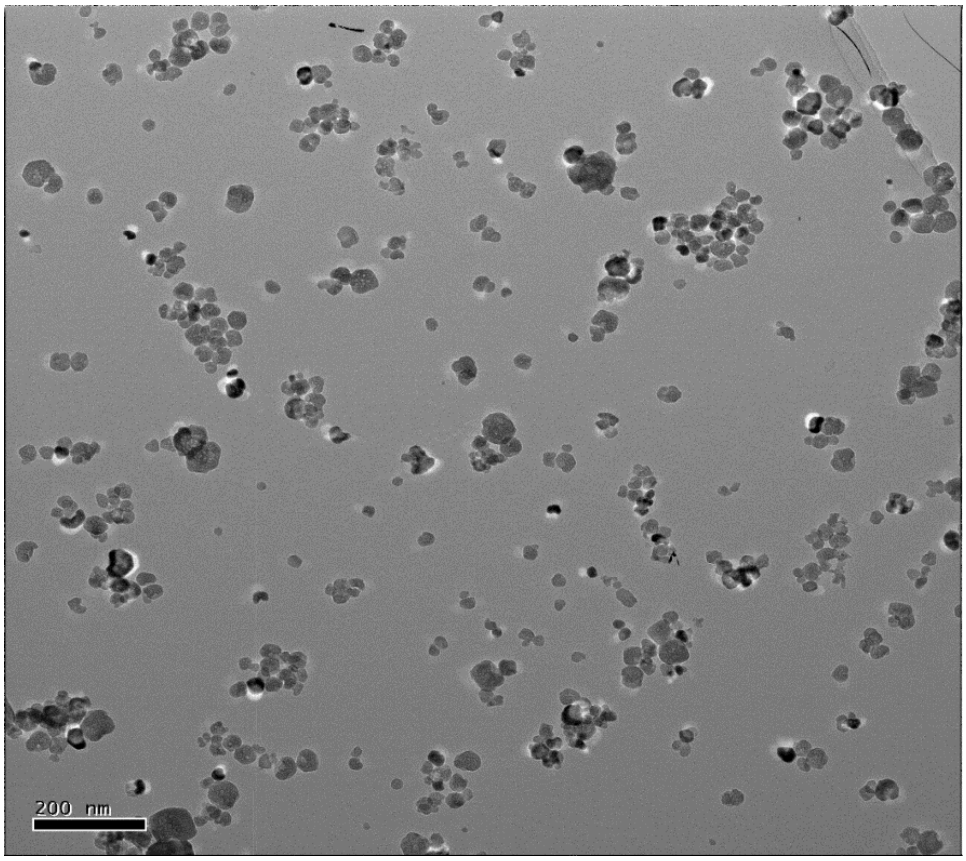

Figure 5.11 TEM image of YAG nanopowder obtained from Process-2

5.6. Compaction and Sintering of YAG nanopowder

5.6.1. Compaction

To fabricate the compact we use YAG nanopowder from process-2 after calcination at 900^{o}C. The uniaxial pressing, cold isostatic pressing (CIP) and the combination of these two are used to make compacts from YAG nanopowders. Compared to the uniaxial pressing, CIP gave more green density due to uniform distribution of applied pressure in all directions. In the present work, the powders are pressed uniaxially and cold isostatically separately to obtain different compacts. After obtaining the compacts, they are conventionally sintered at high temperature. Furthermore, compacts are also prepared by pressure assisted sintering processes like hot pressing, hot isostatic pressing (HIP) and spark plasma sintering (SPS) that combines both consolidation and temperature concurrently.

5.6.2. Sintering

In this work, four different sintering techniques are used to make sintered compacts from the selected YAG nanopowders. Conventional sintering, hot pressing, spark plasma sintering (SPS) and hot isostatic pressing (HIP) are the four different techniques used. Initially, conventional sintering was done at different parameters and schedules to produce 14 different samples as shown in Table 4.3 of experimental section. The microstructure of the sintered pellets are analysed using FESEM and images has been shown in Figure 5.12. In this experiment, silica (SiO_2)is added to all samples as sintering additive to enhance the sintering except YAG 12 to understand the sintering behaviour without additive addition. Pure YAG sintering follows solid state diffusion mechanism. SiO_2 doped YAG is densified by liquid phase sintering mechanism. The melting point of pure YAG is 1930^{o}C. The role of the silica is to form a liquid phase in the YAG matrix during high temperature that helps lowering the sintering temperature, so it is called as liquid phase sintering. A liquid phase starts to form at around 1400^{o}C in SiO_2 added YAG, as a result the density of the sample is enhanced.

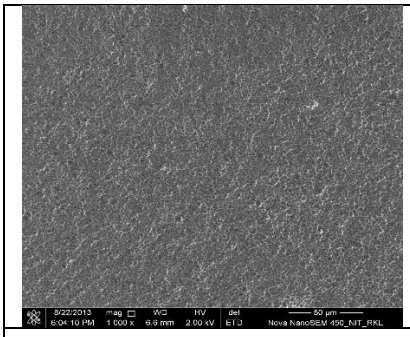	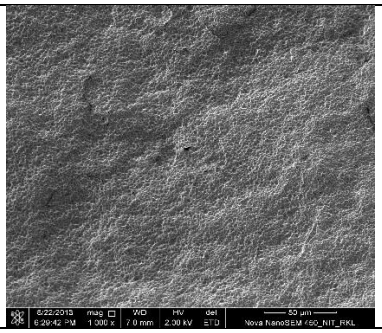	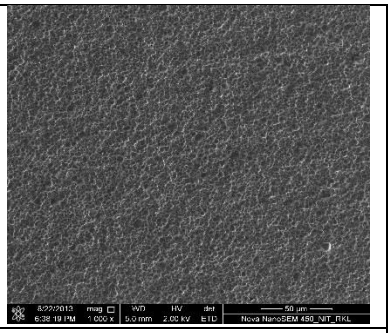
x1000	x1000	x1000
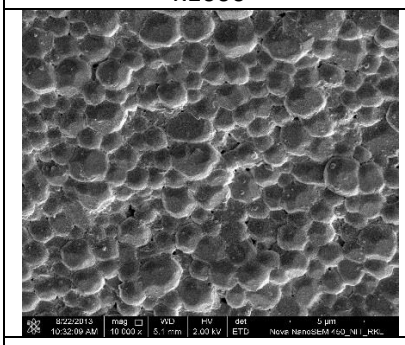	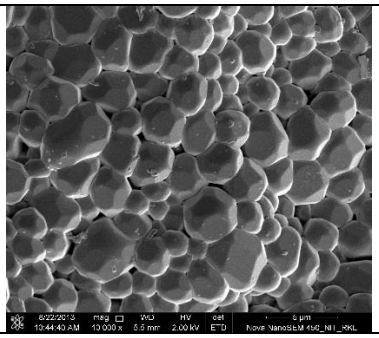	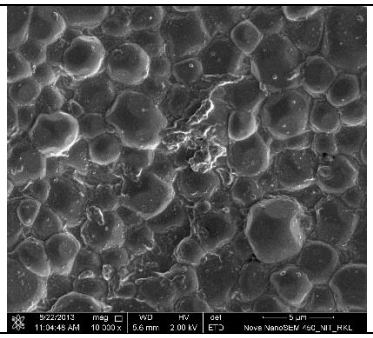
x10000	x10000	x10000
(a) YAG 1	**(b) YAG 2**	**(c) YAG 3**

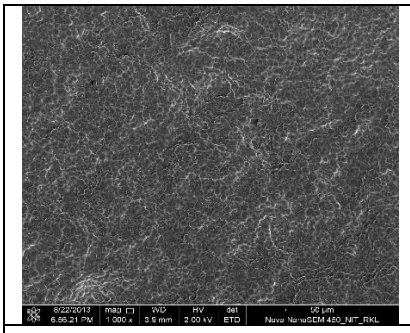	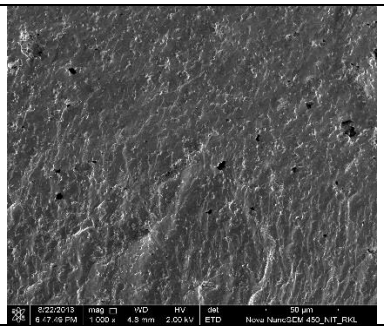	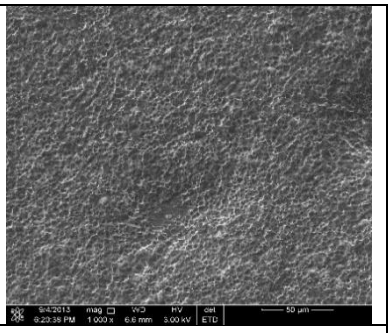
x1000	x1000	x1000
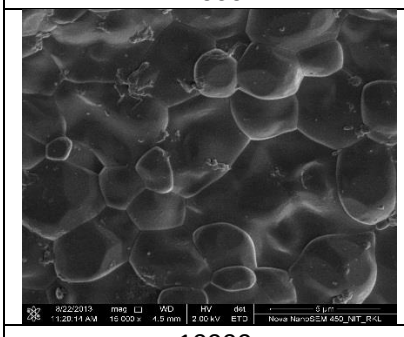	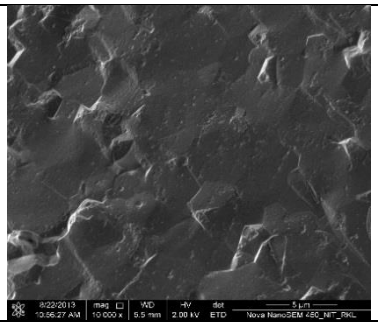	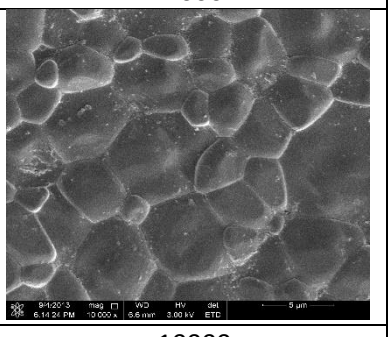
x10000	x10000	x10000
(d) YAG 4	**(e) YAG 5**	**(f) YAG 6**

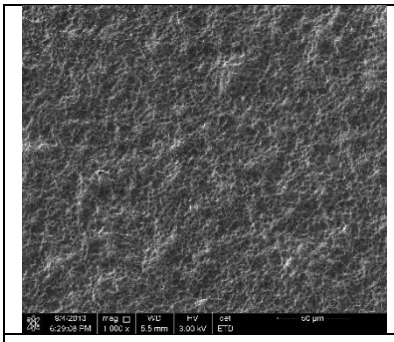	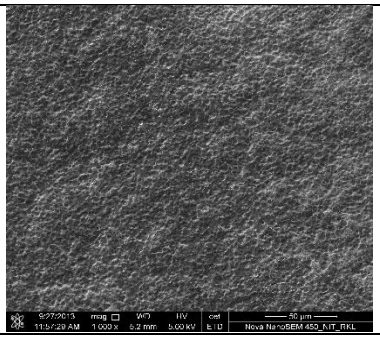	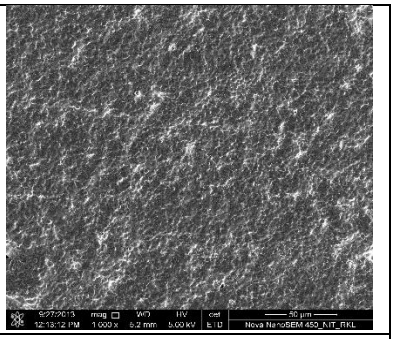
x1000	x1000	x1000
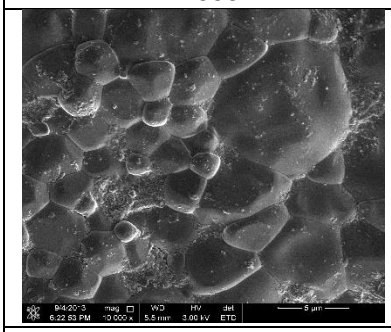	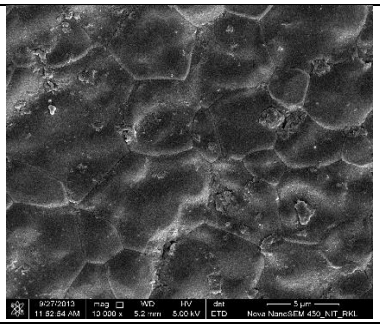	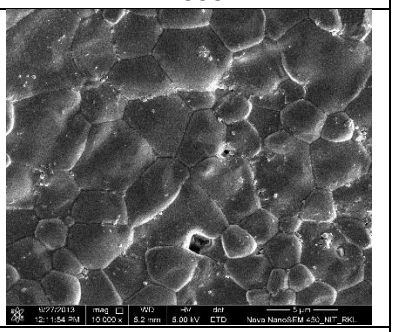
x10000	x5000	x10000
(g) YAG 7	**(h) YAG 8**	**(i) YAG 9**

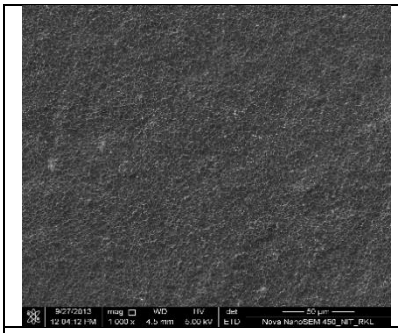	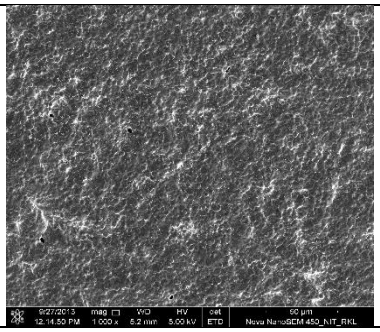	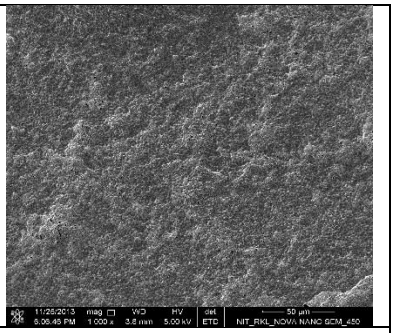
x1000	x1000	x1000
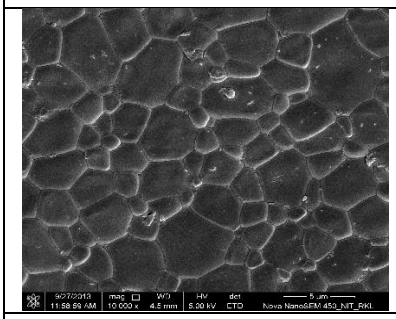	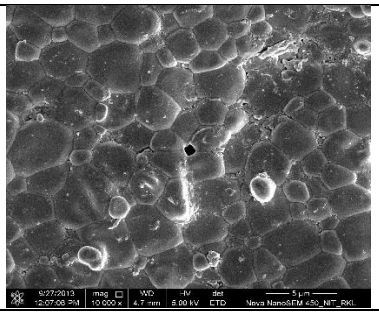	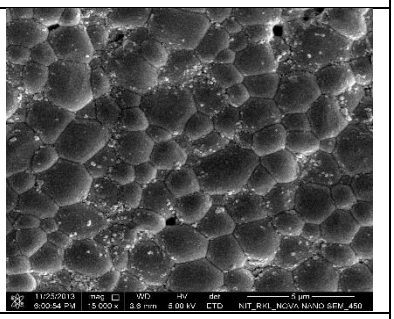
x10000	x10000	x10000
(j) YAG 10	**(k) YAG 11**	**(l) YAG 12**

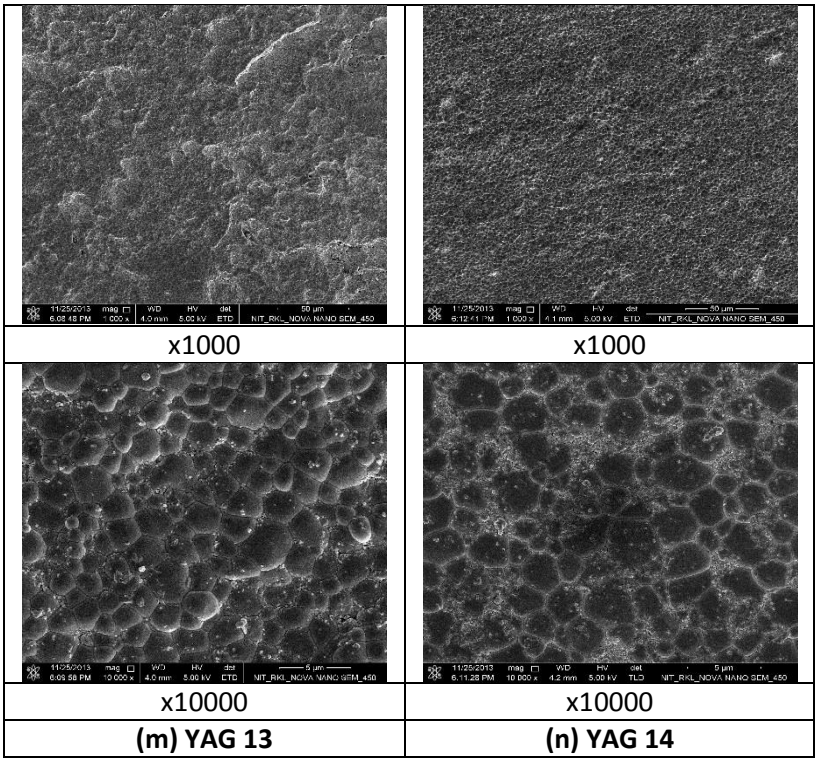

Figure 5.12 FESEM images of sintered pellets

Comparatively, a sample sintered with an optimum amount SiO_2 addition is found to have small grain size than a sample without SiO_2 addition. YAG 12, YAG 13 and YAG 14 are sintered with same sintering parameters like heating rate, holding time and other sintering conditions. These samples contain 0wt%, 0.15wt% and 0.3wt% SiO_2, respectively. A higher grain size is observed for YAG 12 compared to other two samples as seen in Figure 5.12(l), (m) and (n). This is because of the enhanced sintering due to silica addition. But the amount of silica addition has its effect on the transparency of the sintered pellet. If the amount of silica is more, the melted silica makes a thicker layer in between the YAG grains thereby reducing the transparency of sintered sample. A translucent pellet is observed due to excess silica. Presently, the optimum value for SiO_2 additive is 0.5 wt%.

Heating rate affects the grain growth and resulting grain sizes. We have used different heating rate in the conventional sintering process to fabricate sintered pellets. It has been found that high heating rate and extensive soaking time at high temperature makes larger and heterogeneous grains. The larger grained polycrystalline materials tend to have poor strength and low thermal shock resistance than the smaller grained polycrystalline materials. The reduction in the grain size improves mechanical properties of the ceramic material. In this work, nano-size polycrystalline yttrium aluminum garnet powder is used to make the sintered transparent ceramics. The optimized grain size can be achieved from precise sintering conditions together with nano-sized starting powders. From the FESEM images it is clear that heating rate, firing temperature and the holding time are the important factors which affect the grain size. Samples prepared using high heating rate have high grain size and the grain growth is also not uniform. Similarly, higher firing temperature and prolonged holding time also increased the grain size. YAG 2 has been sintered using a heating rate of 8^{o}C/minute showing large and heterogeneous grains as seen from Figure 5.12(b).

Uniaxial pressing of optimized YAG nanopowder followed by atmospheric sintering at 1700^{o}C with a heating rate of 2^{o}C/ minute depicts 97% relative density with average grain size 3µm. Cold isostatic pressing (CIP) of optimized powder followed by atmospheric sintering with a heating rate of 2^{o}C/ minute provides more than 97% relative density and 3.2µm grain and their FESEM images are shown in Figure 5.12 (d) and (e).

FESEM images of the hot pressed sample and spark plasma sintered sample are shown in Figure 5.13(a) and (b), respectively. The grain sizes as seen for hot pressed sample is ~6µm with high porosity which is the largest grain size obtained upon comparing conventional sintering and other sintering processes. This is due to high sintering temperature and high heating rate of 1800^{o}C and 10^{o}C/min, respectively. The grain size of the spark plasma sintered samples is not clearly visible at higher magnification.

Hot Isostatically pressed sample showed less porosity than other sintered samples. In this process, sintering was enhanced by application of external pressure through enhanced diffusion and perhaps by plastic deformation process. The point defects and the line defects produced by oxygen vacancies are reduced by post annealing of the sample. From Table 4.4in experimental section, we have found that highest relative density of 99.63% with average grain size of 2.5 micronis observed for hot isostatically pressed (HIP) sample. Comparatively, spark plasma sintered sample also has high density near to the highest value. A residual void at the triple junction of grain boundary is observed in TEM image of the HIPed sample as shown in Figure 5.14.

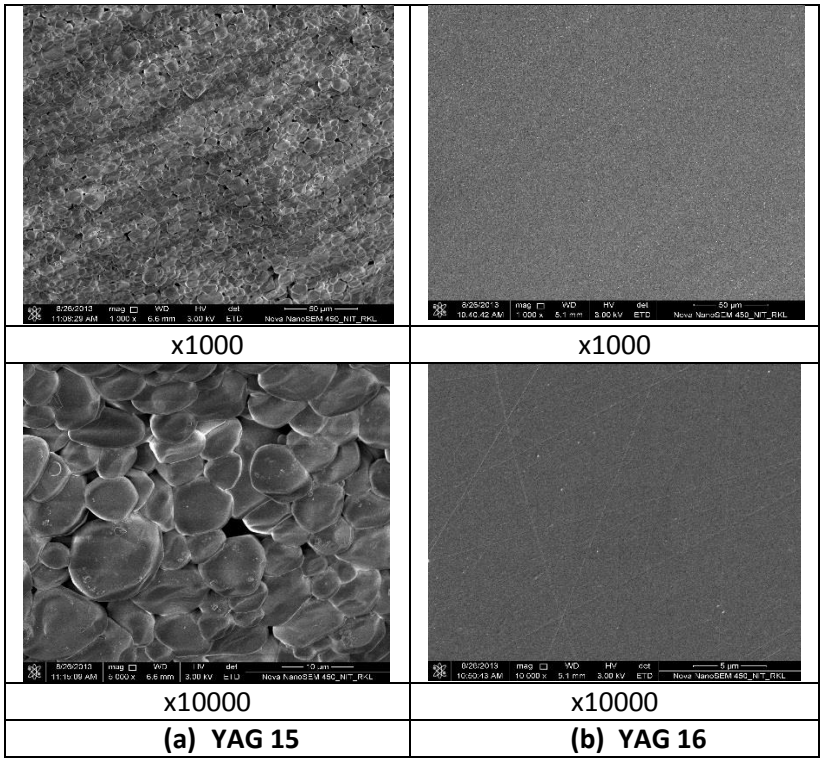

Figure 5.13 FESEM images of hot pressed and spark plasma sintered samples

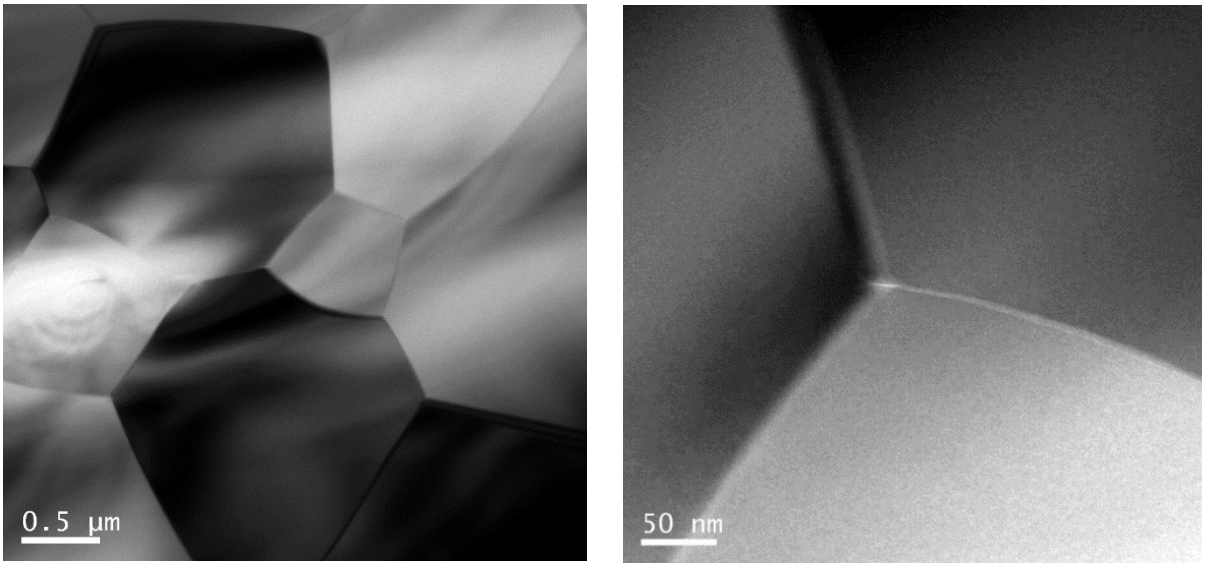

Figure 5.14 TEM images of HIPed sample

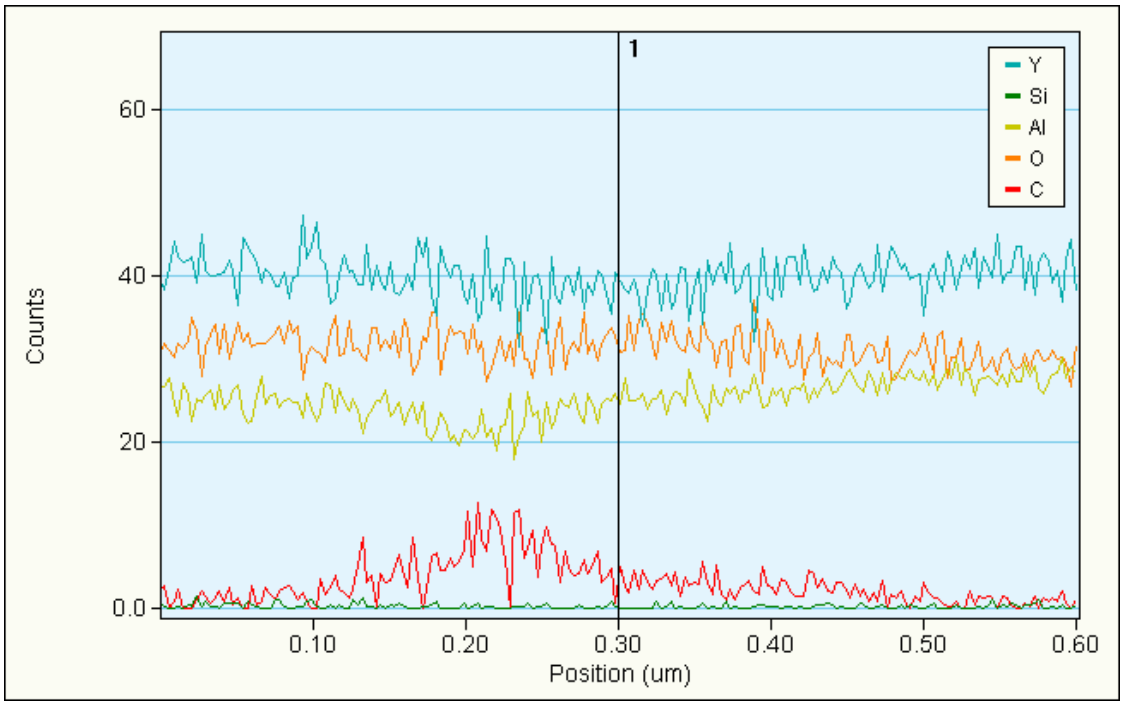

Figure 5.15 TEM-EDS line profile of HIPed sample

Figure 5.15 shows the EDS line profile of hot isostatically pressed sample. It shows the elemental composition at different positions in the sample. Intensity of yttrium, oxygen and aluminium at different positions are plotted. The presence of silica added as sintering additive

is found in very less amount compared to yttrium, aluminium and oxygen amount. Therefore, it has no affect in the YAG phase after sintering. The presence of carbon is due to the sample holder.

5.7. Optical transmittance of HIPed Sample

The optical image and transmission spectra of hot isostatically pressed sample has been shown in Figure 5.16(a) and (b). Transmittance of the sample has been measured for different zone of the sample as shown in Figure 5.16(a). The transparency at various zones in the sintered sample is found different. Maximum transmittance of around 60% is observed at visible region and near infra-red region @ 550nm and 1100nm, respectively. A fairly good transmittance is observed both in the visible and near infra-red region. The transmittance value of the sample is found almost near to the values reported in literature.

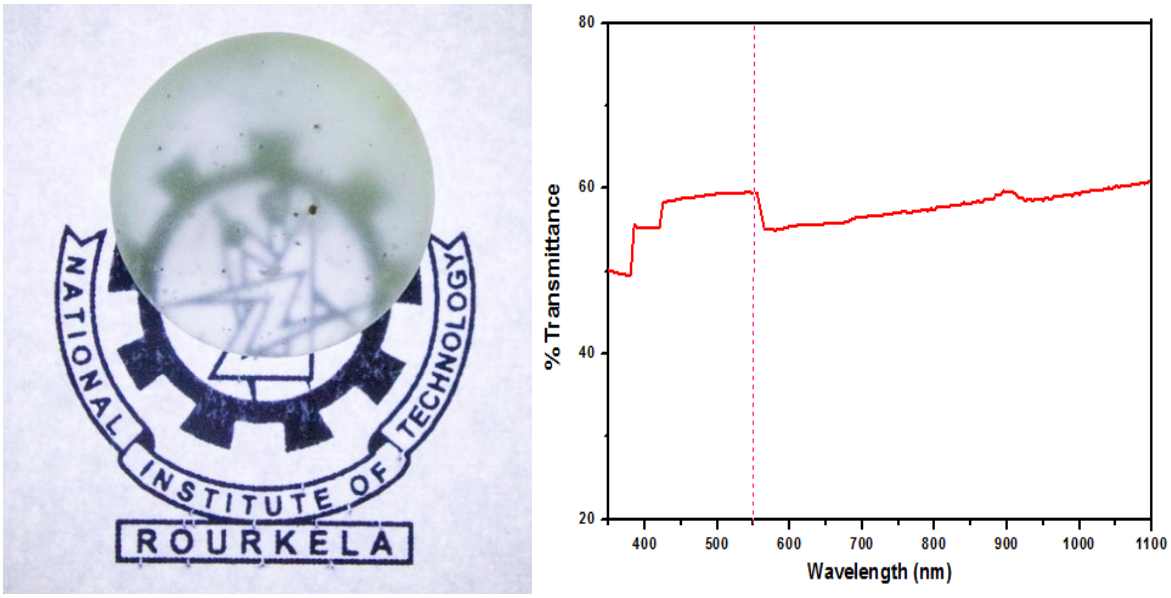

Figure 5.16 (a) Optical Image and (b) Transmission spectra of HIPed sample

Research Highlights

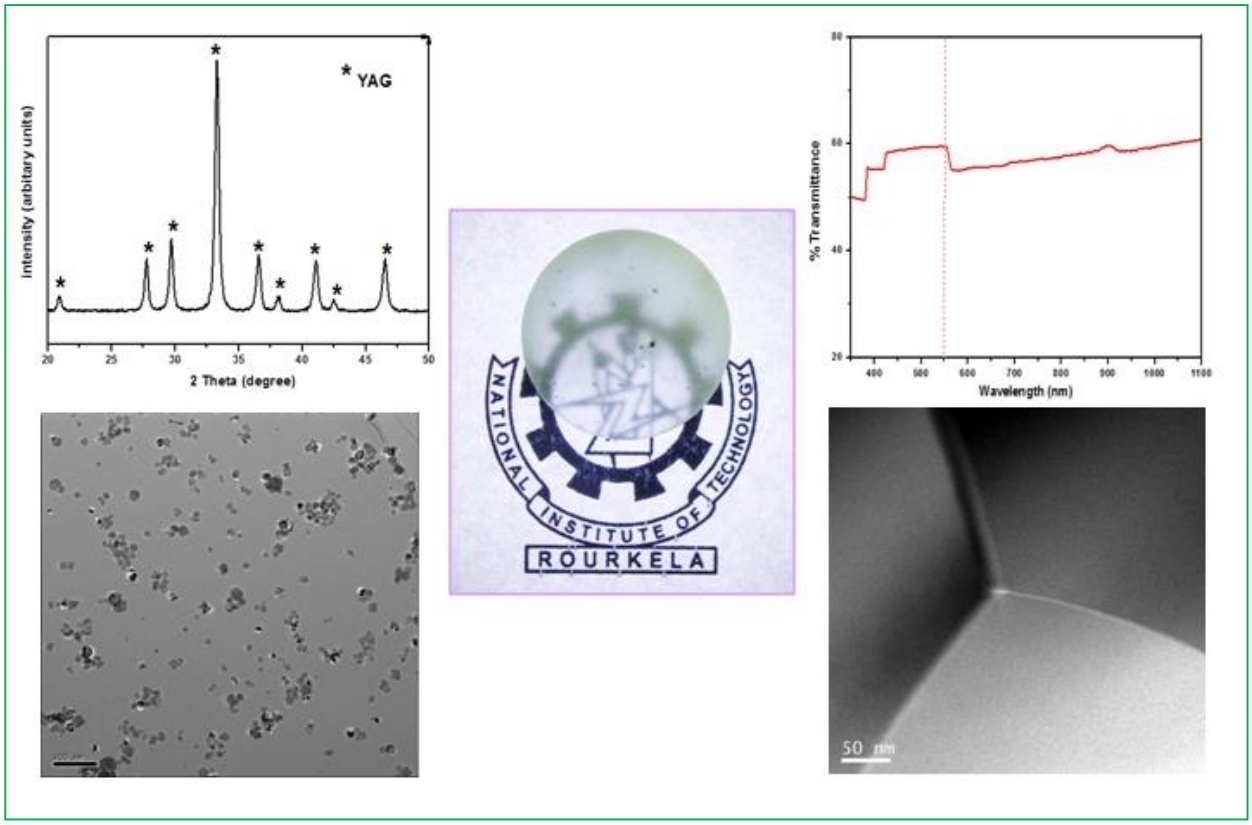

- ✓ Pure 40nm YAG nanoparticles have high degree of crystallinity.
- ✓ Uniaxial pressing and atmospheric sintering followed by hot isostatic pressing develops high dense YAG in presence of silica.
- ✓ YAG disc has 99.6% relative density and 2.5micron grain size.
- ✓ Sintered disc exhibits ~60% transparency in both 550 and 1100nm wavelength

CHAPTER 6

CONCLUSION

6. Conclusion

- The YAG nanopowder obtained from the sol-gel method has very hard agglomeration and low yield.
- Solid state reaction of yttria and alumina requires high temperature to achieve pure YAG phase compared to the other processes. Particle size obtained from solid state reaction process is 260nm and surface area ~5m^2/gm.
- Pure, crystalline and spherical YAG nanopowders with consist of 40nm particle size and surface area of ~34m^2/gm has been synthesized through low temperature co-precipitation process using NH_4HCO_3 as precipitant followed by calcination at 900^oC.
- Uniaxial pressing of optimized powder followed by atmospheric sintering at 1700^oC with a heating rate of 2^oC/ minute depicts 97% relative density with average grain size 3μm.
- Cold isostatic pressing of optimized powder followed by atmospheric sintering with a heating rate of 2^oC/ minute provides more than 97% relative density and 3.2μm grain.
- A large grain (~6μm) size and 93.2% relative density is calculated after hot pressing (HP) YAG nanopowder at 1800^oC with a heating rate of 10^oC/ minute.
- Spark plasma sintered YAG disc exhibits 99.1% relative density when processed at 1300^oC under 60MPa pressure.
- High relative density of 99.63% with average grain size of 2.5μm of translucent disc is found after hot isostatic pressing (HIP) of YAG nanopowder at 1800^oC under 195MPa.
- The hot isostatic pressed sample has maximum transmittance of around 60% in the visible region and near infra-red region of 550nm and 1100nm, respectively.

SCOPE FOR FUTURE WORK

- Preparation of neodymium (Nd) doped powder for laser host transparent ceramics.
- Further densification enhancement through HIP or vacuum sintering of high dense green compact.
- Transparency improvement above 85% in both visible and infrared wavelength.

References

1. F.O. Olsen in Lasers in Materials Processing, ed. E.A. Metzbower, ASM, Metals Park, Ohio, 1983.
2. Xia Li, Hong Liu, Jiyang Wang, Xudong Zhang and Hongmei Cui. “Preparation and properties of YAG nano-sized powder from different precipitating agent”. Optical Materials 25 (2004) 407–412.
3. A. Krell, J. Klimke and T. Hutzler. “Transparent compact ceramics: Inherent physical issues”. Optical Materials 31 (2009) 1144–1150.
4. T. Taira, "RE^{3+}-ion-doped YAG ceramic lasers," IEEE J. Sel. Top. Quantum Electron. 13[3] 798-809 (2007).
5. M. Mizuno and T. Noguchi, Gept. Govt. Ind. Res. Inst. Nagoya, 16, 171 (1967).
6. A. Siegman, Lasers. University Science Books, Mill Valley, CA, 1986.
7. M. Veith, S. Mathur, A. Kareiva, M. Jilavi, M. Zimmer, V. Huch, “Low Temperature Synthesis of Nanocrystalline $Y_3Al_5O_{12}$ (YAG) and Ce-doped $Y_3Al_5O_{12}$via Different Sol-Gel Methods“, Journal of Materials Chemistry 1999, 9, 3069.
8. Vaqueiro P, Lopez-Quintela M A. “Influence of complexing agents and pH on Yttrium-iron garnet synthesized by the sol-gel method”. Chemistry of Materials.1997, 9, 2836-2841.
9. Tokumatsu Tachiwaki, Masaru Yoshinaka, Ken Hirota, Takayasu Ikegami, Osamu Yamaguchi. “Novel synthesis of Y3Al5O12 (YAG) leading to transparent ceramics”. Solid State Communications 119 (2001) 603-606.
10. Ji-Young Park, Seong-Geun Oh, Ungyu Paik, Sei-Ki Moon ,“Preparation of aluminum oxide particles using ammonium acetate as precipitating agent”. Materials Letters, 56 (2002) 429.

11. I. Matsubara, M. Paranthaman, S.W Allison, M.R Cates, D.L Beshears, D.E Holcomb "Preparation of Cr-doped Y3Al5O12 phosphors by heterogeneous precipitation methods and their luminescent properties". Materials Research Bulletin, 35(2000) 217.
12. "Hongzhi Wang, LianGao, Koichi Niihara. Synthesis of nanoscaled yttrium aluminum garnet powder by the co-precipitation method". Materials Science and Engineering: A288(2000) 1.
13. Sordelet DJ, Akinc M, Panchula ML, Han Y, Han MH. "Synthesis of yttrium aluminum garnet precursor powders by homogeneous precipitation". Journal of the European Ceramic Society 14, 1994, 123–130.
14. Masashi Inoue, Hiroyuki Otsu, Hiroshi Kominami and Tomoyuki Inui. "Synthesis of Yttrium Aluminum Garnet by the Glycothermal Method". Journal of the American Ceramic Society. 74 (6) (1991) 1452.
15. Nyman M, Caruso J, Hampden Smith MJ. "Comparison of solid-state and spray-pyrolysis synthesis of yttrium aluminate powders". Journal of the American Ceramic Society 80,(1997) 1231–1238.
16. Zhou YH, Lin J, Yu M, Han SM, Wang SB, Zhang HJ. Morphology control and luminescence properties of YAG:Eu phosphors prepared by spray pyrolysis. Material Research Bulletin38, (2003) 1289–99.
17. Li J, Pan YB, Qiu FG, Wu YS, Guo JK. "Nanostructured Nd:YAG powders via gel combustion: the influence of citrate to nitrate ratio". Ceramic International 34 (2008) 141–9.
18. Chen DY, Jordan EH, Gell M. "Sol–gel combustion synthesis of nanocrystalline YAG powder from metal-organic precursors". Journal of the American Ceramic Society 91 (2008) 2759–62.

19. Li J, Pan YB, Qiu FG, Wu YS, Liu WB, Guo JK. “Synthesis of nanosized Nd:YAG via gel combustion”. Ceramic International 33(2007) 1047–52.
20. R. Boulesteix, A. Maître, J.-F. Baumard, C. Sallé, Y. Rabinovitch. “Mechanism of the liquid-phase sintering for Nd:YAG ceramics”. Optical Materials (2008).
21. LI Chang-qing, ZUO Hong-bo, ZHANG Ming-fu, HAN Jie-cai and MENG Song-he. “Fabrication of transparent YAG ceramics by traditional solid-state-reaction method”. Trans. Nonferrous Met. SOC. China 17(2007) 148-153.
22. Ming-Shyong Tsai, Wen-Chuan Fu, Wen-Chang Wu, Cheng-Ho Chen and Chien-Hsin Yang. “Effect of the aluminum source on the formation of yttrium aluminum garnet (YAG) powder via solid state reaction”. Journal of Alloys and Compounds 455 (2008) 461–464.
23. L.B. Kong, J. Ma and H. Huang. “Low temperature formation of yttrium aluminum garnet from oxides via a high-energy ball milling process”. Materials Letters 56 (2002) 344–348.
24. Qiwu Zhang and Fumio Saito. “Mechanochemical solid reaction of yttrium oxide with alumina leading to the synthesis of yttrium aluminum garnet”. Powder Technology 129 (2003) 86– 91.
25. Yongming Zhang and Hongming Yu. “Synthesis of YAG powders by the co-precipitation method”, Ceramics International 35 (2009) 2077–2081.
26. Jiang Li, Feng Chenb, Wenbin Liu, Wenxin Zhang, Liang Wang, Xuewei Ba, Yingjie Zhu, Yubai Pan and JingkunGuo . “Co-precipitation synthesis route to yttrium aluminum garnet (YAG) transparent ceramics”. Journal of the European Ceramic Society 32 (2012) 2971–2979.
27. Ji-Guang Li, Takayasu Ikegami, Jong-Heun Lee, Toshiyuki Mori and Yoshiyuki Yajima. “Co-precipitation synthesis and sintering of yttrium aluminum garnet (YAG)

powders: the effect of precipitant". Journal of the European Ceramic Society 20 (2000) 2395-2405

28. Caroline Marlot, Elodie Barraud, Sophie Le Gallet, Marc Eichhorn and Frederic Bernard. "Synthesis of YAG nanopowder by the co-precipitation method: Influence of pH and study of the reaction mechanisms". Journal of Solid State Chemistry 191 (2012) 114–120.
29. Xianxue Li, Bingyun Zheng, Tareque Odoom-Wubah and Jiale Huang. "Co-precipitation synthesis and two-step sintering of YAG powders for transparent ceramics". Ceramics International 39(2013)7983–7988.
30. Yuanhua Sang, YaohuiLv, Haiming Qin, Xiaolin Zhang, Hong Liu, Jiyang Wang, Xudong Sun and Robert I. Boughton. "Chemical composition evolution of YAG co-precipitate determined by pH during aging period and its effect on precursor properties". Ceramics International 38 (2012) 1635–1641.
31. Shaokang Yang, WenxiuQue, Jin Chen and W.G. Liu. "Nd:YAG nano-crystalline powders derived by combining co-precipitation method with citric acid treatment". Ceramics International 38 (2012) 3185–3189.
32. Q.X. Zheng, B. Li, H.D. Zhang, J.J. Zheng, M.H. Jiang and X.T. Tao. "Fabrication of YAG mono-dispersed particles with a novel combination method employing supercritical water process". J. of Supercritical Fluids 50 (2009) 77–81.
33. Prabhu Ramanujam, Bala Vaidhyanathan, Jon Binner, Aashu Anshuman and Chris Spacie. "A comparative study of the synthesis of nanocrystalline Yttrium Aluminium Garnet using sol-gel and co-precipitation methods". Ceramics International 40 (2014) 4179–4186.

34. Lin Yang, Tiecheng Lu, Hui Xu and Nian Wei. “Synthesis of YAG powder by the modified sol-gel combustion method”. Journal of Alloys and Compounds 484 (2009) 449–451.
35. Zhihong Sun, Duorong Yuan, Haoqiang Li, XiulanDuan, Haiqing Sun, Zengmei Wang, Xuecheng Wei, Hongyan Xu, Caina Luan, Dong Xu and Mengkai Lv. “Synthesis of yttrium aluminum garnet (YAG) by a new sol-gel method”. Journal of Alloys and Compounds 379 (2004) L1–L3.
36. Kwadwo A, Appiagyei, Gary L. Messing and John Q. Dumm. “Aqueous slip casting of transparent yttrium aluminum garnet (YAG) ceramics”. Ceramics International 34 (2008) 1309–1313.
37. Fei Tang, Yongge Cao, Jiquan Huang, Wang Guo, Huagang Liu, Qiufeng Huang and Wenchao Wang. “Multilayer YAG/Re:YAG/YAG laser ceramic prepared by tape casting and vacuum sintering method”. Journal of the European Ceramic Society 32 (2012) 3995–4002.
38. HUANG Yihua, JIANG Dongliang, ZHANG Jingxian, LIN Qingling and HUANG Zhengren. “Sintering of transparent Nd:YAG ceramics in oxygen atmosphere”. Journal of Rare Earths, Vol. 31, No. 2, Feb. 2013, P. 153.
39. Sunipa Bhattacharyya, T.K. Mukhopadhyay, Kausik Dana and SankarGhatak. “Pressureless reaction sintering of yttrium aluminium garnet (YAG) from powder precursor in the hydroxyhydrogel form”. Ceramics International 37 (2011) 3463–3468.
40. M. Suárez, A. Fernández, J.L. Menéndez, M. Nygren, R. Torrecillas and Z. Zhao. “Hot isostatic pressing of optically active Nd:YAG powders doped by a colloidal processing route”. Journal of the European Ceramic Society 30 (2010) 1489–1494.

41. Wei Zhang, Tiecheng Lu, Benyuan Ma, Nian Wei, Zhongwen Lu and Feng Li. “Improvement of optical properties of Nd:YAG transparent ceramics by post-annealing and post hot isostatic pressing”. Optical Materials 35 (2013) 2405-2410.
42. RachmanChaim, Michael Kalina and James Z. Shen. “Transparent yttrium aluminum garnet (YAG) ceramics by spark plasma sintering”. Journal of the European Ceramic Society 27 (2007) 3331–3337.
43. NaumFrage, Sergey Kalabukhov, NataliyaSverdlov, Vladimir Ezersky and Moshe P. Dariel. “Densification of transparent yttrium aluminum garnet (YAG) by SPS processing”. Journal of the European Ceramic Society 30 (2010) 3331–3337.
44. Giulia Spina, Guillaume Bonnefont, Paola Palmero, Gilbert Fantozzi and Jérome Chevalier. “Transparent YAG obtained by spark plasma sintering of co-precipitated powder. Influence of dispersion route and sintering parameters on optical and microstructural characteristics”. Journal of the European Ceramic Society 32 (2012) 2957–2964.
45. N. Frage, S. Kalabukhov, N. Sverdlov, V. Kasiyan, A. Rothman and M.P. Dariel. “Effect of the spark plasma sintering (SPS) parameters and LiF doping on the mechanical properties and the transparency of polycrystalline Nd-YAG”. Ceramics International 38 (2012) 5513–5519.
46. Wenbin Liu, Yanping Zeng, Jiang Li, Yu Shen, Yong Bo, Nan Zong, Pengyuan Wang, Yiding Xu, Jialin Xu, Dafu Cui, Qinjun Peng, Zuyan Xu, Di Zhang and Yubai Pan. “Sintering and laser behavior of composite YAG/Nd:YAG/YAG transparent ceramics”. Journal of Alloys and Compounds 527 (2012) 66– 70.
47. Jing Li, Qiang Chen, Guoying Feng, Wenjuan Wu, Dingquan Xiao and Jianguo Zhu. “Optical properties of the polycrystalline transparent Nd:YAG ceramics prepared by two-step sintering”. Ceramics International 38S (2012) S649–S652.

48. M. Suárez, A. Fernández, J.L. Menéndez,R. Torrecillas, H. U. Kessel, J. Hennicke,R. Kirchner and T. Kessel. “Challenges and Opportunities for Spark Plasma Sintering: A Key Technology fora New Generation of Materials”.